FACULTY OF ENGINEERING TECHNOLOGY

BACHELOR THESIS

MODELLING THE HYDRODYNAMIC EFFECTS OF THE CONSTRUCTION OF A SMALL ISLAND NEAR THE WADDEN SEA

YING ZHOU

EXTERNAL SUPERVISOR

N. GELEYNSE PHD

INTERNAL SUPERVISOR

DR. IR. P.C. ROOS

MARCH 2023

WATER PROOF

UNIVERSITY OF TWENTE.

University of Twente
Faculty of Engineering Technology
De Horst 2
7522 LW Enschede
The Netherlands
https://www.utwente.nl/

WaterProof
Marine Consultancy & Services B.V.
IJsselmeerdijk 2
8221 RC, Lelystad
The Netherlands
https://waterproofbv.com/

PREFACE

This thesis report marks the end of my bachelor Civil Engineering at the University of Twente. I investigated the hydrodynamic effects of the construction of a small island near the Wadden Sea using the numerical modelling tool Delft3D-SWAN. This research was performed at WaterProof. During my time there I learned to apply the knowledge that I have obtained over the course of my bachelor. Next to that, I also learned a lot of new things that were exciting and motivate me to continue my career in this field.

A special thanks to my supervisors Nathanaël Geleynse and Koen van der Laan for their guidance, feedback, and support. Their insights and observations really helped me get a better understanding of the underlying theory. I would also like to thank my internal supervisor Pieter Roos for his guidance and feedback, especially during the early stages of my thesis. Finally, I want to thank my colleagues who have read through my draft reports and provided me with feedback.

And lastly, I hope you enjoy reading my thesis report and please feel free to contact me if any questions arise.

Ying Zhou
y.zhou-6@student.utwente.nl

March, 2023

TABLE OF CONTENTS

SUMMARY

This study investigates the hydrodynamical effects of a small energy island in the eastern Dutch coastal waters. This energy island is part of an ongoing investigation to accommodate wet infrastructure (cables, pipelines, etc) that connects offshore windfarms to the main land.

The study area is located near the mouth of the Ems estuary, west of the German barrier island 'Borkum' and north of the Dutch Wadden barrier island 'Rottumeroog'.

The seabed of the study area is locally very dynamic, with areas where the seabed has seen variations of as much as 10 m in about 40 years. The seabed mobility is of importance to the selection of the optimal location of the foreseen energy island. Even though parts of the shoal on which the island is planned to be built (the Ballonplaat) has been relatively stable the past few decades, it is yet not unknown whether this will be the case in the future. Additionally, the hydrodynamics in the area can be quite severe, especially during winter storms with high waves. These overall characteristics of the study area are described in chapter 2 along with some theory concerning waves as waves are the major forcing that is active in the area, along with the tidal currents.

To minimize the impacts of the energy island, adjustments can be made to the design and features. Some examples of these features are the shape and orientation of the island. Island designs and features are presented and discussed in chapter 3, where it is also explained how a specific island design can be implemented to a Delft3D model. By modelling various island designs, the effects on the flow and waves in the area is studied. The output of computations with an existing Delft3D model of the Wadden Sea and Ems estuary is used for the analysis.

The main parameters and assumptions underlying the Delft3D model are discussed in chapter 4. In this chapter, the computed currents for the situation without an island are also presented. Furthermore , a comparison is made between the waves that are computed with a 2D SWAN model along a given transect and computations that were done in this study with several theoretical 1D wave models for the same seabed profile along the transect as well as for simpler linear bed profiles.

The simulations with the Delft3D-SWAN model showed the effects of an island on the depth-averaged current velocity patterns and significant wave height, which are discussed in chapter 5. The results show that, while the addition of an island presents clear changes in the flow patterns, the impact on the significant wave height is relatively small. The individual effects of the island parameters, including size and orientation, are also investigated, but revealed to be difficult to consider independently.

1. INTRODUCTION

With the ever-growing demand for sustainable and renewable energy sources, mainly caused by the effects of climate change, the interest in wind power is also increasing. Along with solar energy, wind turbines are one of the more popular ways of generating renewable energy. With the growing number of onshore windfarms, a densely populated country like the Netherlands would soon run out of space to install these turbines. Additionally, many residents do not want such a massive structure near their residence because of its noise and impact on the landscape. Another option is to built wind farms offshore, which is being done increasingly. The energy generation at sea is generally higher than onshore because of the greater wind speeds. Furthermore, the windfarms can be built on a larger scale and the public will be less impacted than when they are built on land.

However, since all this energy is being generated at sea, this energy needs to be transported to the onshore grid before it can be used. This is done by transmission cables that are buried into the seabed, but one of the big challenges is the distance these cables have to cross. A novel solution to this is the construction of artificial so-called energy islands that serve as hubs or green power plants (The Danish Energy Agency, n.d.). By connecting the offshore wind farms to the onshore electricity grid through such an island, the wind farms can also be built farther away at sea. However, it can be expected that such an artificial island greatly impacts the environment around it, like hydrodynamic elements such as water depth, currents, and waves, or morphodynamic components such as seabed mobility, sediment transport, and channel migration.

This research will focus on the eastern Dutch Wadden Sea area, where several cable routes are already running through (WaterProof, 2022). Several studies have previously been conducted on exploration of the area, cable route alternatives, and cable coverage. This study will look at the effects of the construction of an island on the hydro- and morphodynamic developments in the area.

1.1 CONTEXT

In this section the context of the project will be outlined through the research motivation, problem statement, and research field where relevant results of previous studies will be discussed.

1.1.1 Research Motivation

Currently, the energy transition has prompted the Netherlands to invest heavily in the development of offshore windfarms. The energy that is being generated by these windfarms is transported onshore by means of cables that are buried into the seabed. To extend the range of these cables, so-called energy islands can be constructed thereby allowing bigger windfarms to be built further offshore, which in turn can generate more energy. In order to gather the energy on the island, the cables will be put through a tunnel that connects the island to the onshore grid. Additionally, by building a tunnel that can fit multiple cables, more energy can be distributed while the tunnel also serves as a last resort protective layer. The cables should be buried deep enough such that they are protected against external threats like fishing gear and dragged non holding anchors (WaterProof, 2022). However, the construction of such an island and tunnel will have a big impact on the surrounding environment, including the seabed. When the seabed is dynamic, the sediment from the protective layer of the cables can gradually disperse or accumulate. When the layer disperses, the cables, or in this case the tunnel, could get exposed, possibly leading to a lot of trouble. To be safe, the cables could be buried much deeper than is required, however, this leads to unnecessary costs and inefficiency. When the cables are buried too deep, heat that gets generated cannot dissipate and the cables get overheated. Aside from this being damaging to the cables, power loss can occur, which would defeat the purpose of building new windfarms farther offshore to generate more energy.

This assignment is performed at WaterProof. It is commissioned by, and part of a continuing research for TenneT.

1.1.2 Problem Statement

As part of the design of the route along which these type of cables are being installed, hydro-morphological research is being done by companies such as WaterProof. Since the concept of energy islands is relatively novel, not much is known about the effects of such islands, especially in this study area (just north of the eastern Dutch Wadden Sea, at the mouth of the Ems estuary). Using the numerical modelling tool Delft3D coupled with SWAN, this research will identify what the natural environment in the area is currently, and how it changes after the construction of an artificial island. This includes the strength of the sea currents and waves.

1.1.3 Research Field

This section discusses what is known about the hydro- and morphodynamic effects of artificial islands, and also present what is yet unknown.

Previous studies on artificial islands

The coastal effects of the construction of artificial islands were investigated in previous studies. Compared to Europe, construction of new islands is more common in Asia and the Middle East (Chee, Othman, Sim, Mat Adam, & Firth, 2017), often with the main purpose of accommodating the growing population. Examples are a case study by Li et al. (2022) on the impact of artificial islands on beach stability of sandy shores in southern China, and a study by Guo et al. (2018) which uses a semi-implicit Lagrangian-Eulerian finite difference method to simulate the hydrodynamic effects of an artificial island off the south-eastern coast of China. Two more cases in Israel and China will be discussed in more detail below.

Artificial islands along the coast of Israel

Deltares (1999) previously conducted a study on the “morphological impacts due to the construction of artificial islands along the coast of Israel”. This study assessed 3 so-called island schemes at 3 different locations along the coast of Israel. It is mentioned that in a previous study Lievense et al. (1994) discussed and evaluated an island shape, which resulted in a preference for a “teardrop”. The orientation of the axis of the teardrop is towards the incoming local wave direction to minimise coastal impact. The 3 schemes were “airport island scheme off Tel Baruch”, “single island scheme off Bat Yam”, and “triple island scheme off N.Herzliya”. The shapes of these schemes can be seen in the Figure 1, respectively.

The study looked at local, as well as regional impacts regarding the seabed (local scour and regional lowering or raising) and coastal erosion or deposition of the beach on either side of the schemes. The software that was used for the modelling was UNIBEST for the schematised coastline modelling and Delft3D(2Dh) for a more detailed morphological evaluation, both developed by Deltares (Delft Hydraulics at the time).

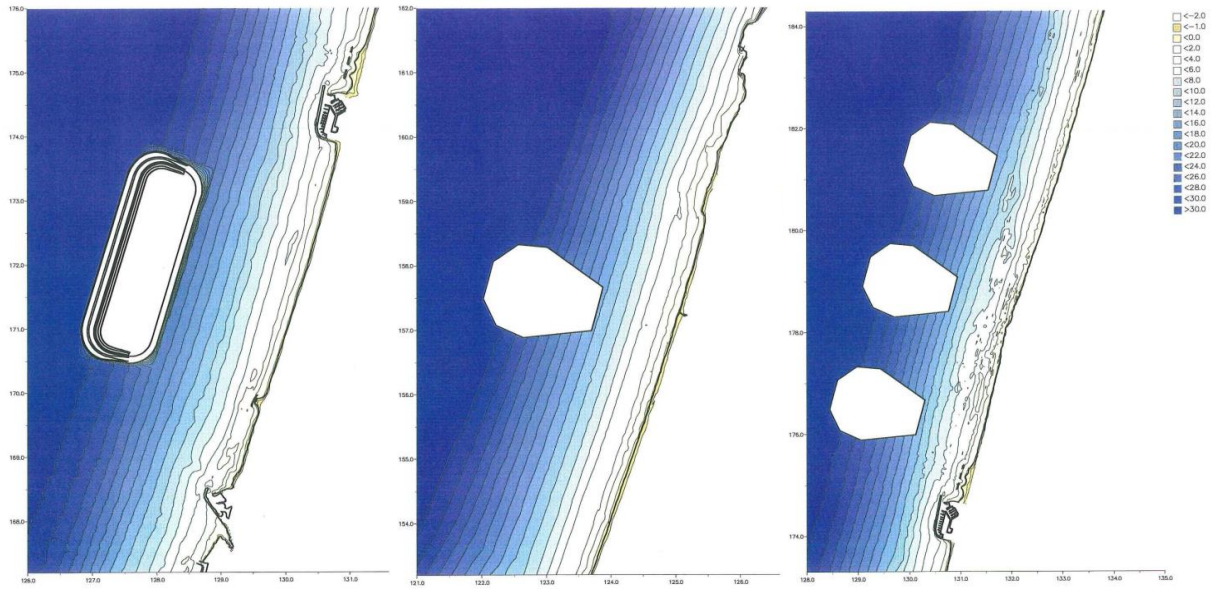

Figure 1 From left to right: airport island alternative (1:40000), single island alternative at Bat Yam (1:40000), and triple island alternative north of Herzliya (1:50000).

After deciding on the island layout, the existing situation without islands was first modelled, then the island layouts without any additional measures, and finally the islands with mitigating measures to reduce the effects of the disturbances created by the tested layouts. The model was simulated in 3 phases with conditions: 0-15 years with an average annual scenario, at the start of year 15 with a 2-day 1:25 year storm, and 15-30 years with average annual conditions. The results and conclusions that followed from the simulations are listed below.

- Even in the absence of an island scheme the foreshore profile is still steepening in the areas off Herzliya itself and off Apollonia leading to increased vulnerability, particularly in storm events.
- Direct coastal erosion impacts can be successfully mitigated by adding measures comprising of offshore breakwaters
- For all layouts some foreshore erosion that occurs in the existing situation will slightly worsen in case of an island
- Severe erosion impacts are to be expected onto the foreshore and eventually also to the shoreline to the north, but these impacts can be mitigated by adding measures

The study emphasises that cliff erosion mechanisms were not properly modelled, meaning that cliff erosion rates could not be shown as a model result. This is explicitly mentioned for the airport island and triple island scheme, but also in the existing situation (without islands), the cliffs on the coast show a tendency for erosion. This is of concern because a deeper foreshore area, especially in front of a cliff coast, will allow for larger waves to reach the coast. The authors recommend regular monitoring, as the cliffs are showing a tendency for erosion in the existing situation without islands.

Mega offshore artificial island (MOAI) in the south of China

Another paper analysed the coastal changes of a 8 km long beach to get insight into potential morphological feedback to a MOAI in the south of China. In April 2016, a large scale project to create a MOAI was completed, resulting in an artificial island with a diameter of approximately 2.3 km, roughly 1.9 km from the nearest coast. The island layout is shown in Figure 2.

The mean tidal range at the local coast is 1.18 m, with the coastal tides being irregular diurnal and microtidal. Furthermore, waves are mainly induced by local winds, rather than swells. In the winter,

the waves mainly move from east-northeast and northeast, while in summer seasons they move from northeast and northwest. The averaged significant wave height was found to be 0.5 m in 2014. The shoreline changes after the construction of a MOAI are visualised in Figure 2 below.

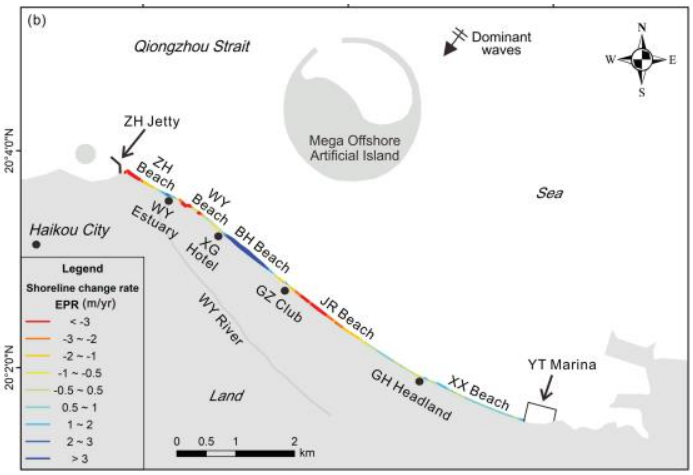

Figure 2 Shoreline change between 2011 (pre-MOAI) and 2019 (post-MOAI) where blue indicates accretion (Liu, et al., 2022).

The visualisation for beach profile changes looks somewhat similar to the shoreline change, but the values seem a bit more extreme where ZH and WY Beach are both coloured red and XX Beach dark blue, while JR Beach is more yellow overall. Next, a similar result was shown for the coastal bed-level changes after the MOAI construction with a dynamic stability or slight retreat for XX Beach, moderate retreat at JR Beach, notable accretion at BH Beach, and dramatic retreat at WY and ZH Beach.

Liu et al. (2022) concluded that the construction of such an MOAI had a direct impact on the shoreline position and profile morphology, while also greatly changing the longshore sediment transport patterns along the coast. They suggest that the variation in longshore sediment transport patterns may be explained by oceanographic processes. Where the waves before the presence of the MOAI mainly came from NE perpendicular to the shoreline, there is a lot more variation now. This is illustrated in the figure below.

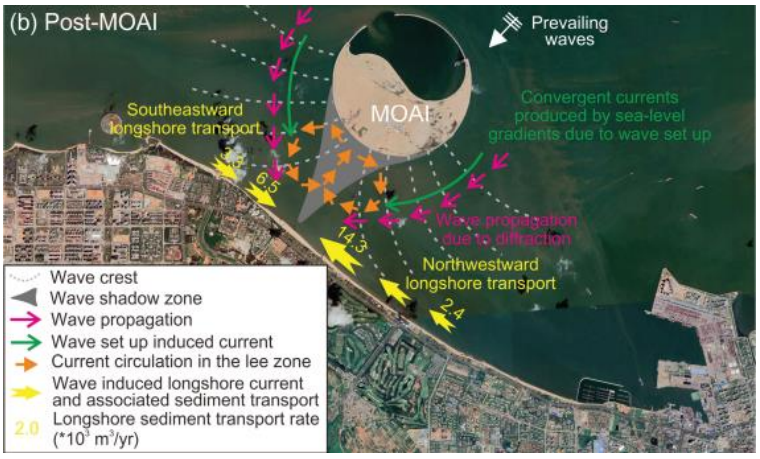

Figure 3 Conceptual model of the oceanographic processes after the construction of the MOAI (Liu, et al., 2022).

As can be seen, a much more intricate pattern appeared which created a more complex system. However, Liu et al. (2022) mention that other factors may also be responsible for the morphological variation, such as typhoons and climate change.

1.2 RESEARCH OBJECTIVE AND QUESTIONS

The objective of this study is, with a model based research (Delft3D-SWAN), to determine the possible effects of the construction of a small island north of the eastern Wadden Islands on the hydrodynamic developments in the area.

To fulfil the research objective some questions should be answered. The first question is meant to get familiar with the area before further research can be done. This was partially done in preparation of the assignment when writing the proposal. From literature research (described in section 2.1), it can be concluded that the area (the eastern Dutch Wadden Sea) is quite dynamic and has many different factors that are relevant to consider. Thus the following question can be asked:

1. What are the current morphological and hydrodynamic conditions in the area without an artificial island?

Essential to the main objective of the research are the island designs that will be tested. Therefore, the next question should be answered as well.

2. What are possible designs for an island and which island features can be distinguished and varied?

Next, the research will be mainly built on the results from a Delft3D-SWAN model, so it is important to also get familiarized with the model. The question that is relevant for this is:

3. How is the Delft3D-SWAN model constructed and what are the main model settings?

This research question can be supported by the next sub-questions:

   a. Which assumptions are being made?
   b. How can an artificial island be added into Delft3D/SWAN?
   c. How does the SWAN model compare to a theoretical wave model?

Finally, a crucial question to ask that will help reach the research objective can be expressed in the following way:

4. What are the hydrodynamic responses in the study area resulting from the addition of an island and which island feature is most influential in affecting the hydrodynamics?

1.3 METHODOLOGY

The study is divided into five phases:

- The first phase is focused on getting familiar with the study area.

This will be done by means of a literature study, consisting of reviewing several reports on the morphological developments in the area, possibly complimented with an analysis of recent morphological developments based on an analysis of seabed charts. Information will primarily be drawn from 2 previous reports from WaterProof (2021 and 2022) that studied the same area, with additional reports for supportive information.

- In the second phase, possible designs of an island are explored.

Variables such as location, water depth, area, and shape of the island are considered and combined. This will then be added to the model to make calculations possible.

- In the third phase, a pre-existing numerical Delft3D-SWAN model will be used and extended to calculate the water levels, sea currents and waves in the study area, without an island.

This phase is primarily meant for developing knowledge and understanding of such a mathematical model. After this, the results will be compared with available measurement data to calibrate the model. Next to the water levels and currents, waves will also be calculated with the (more expanded) model in this phase. Input data for the base of the model is the bathymetry of the area, which was survey data from Rijkswaterstaat in the previous study (WaterProof, 2021). Furthermore, boundary conditions of the modelled area should be taken into account. Finally, considering the model will be in line with the previous research, the following parameters, amongst others, are expected to be encountered: wave period, amplitude, length and celerity.

- In the fourth phase, a comparison is made between the results of the SWAN wave model and the theoretical wave model.

In this phase, a simplified 1D wave model including shoaling, refraction, bottom friction and wave breaking will be put together in Excel. The wave height results of this simplified model will be compared to the results obtained from the 2D SWAN model.

- In the fifth and final phase calculations will be performed with which results on the effects of an island on the previously computed currents and waves will be obtained.

This will be done for the several island designs that have been created in the previous phase. With the results of these computations, a recommendation can be given on the design which minimizes the effect of the island on the present-day hydro- and morphodynamics in the area.

1.4 REPORT STRUCTURE

The report is structured as follows. Chapter 2 will explore relevant background information about the study area as well as some wave theory underlying the SWAN wave model that is of importance especially for the comparison with the theoretical wave models. Chapter 3 will explain the island designs, how a selection was made, and how it was implemented in the model. Next, chapter 4 will discuss the model settings and the first results without an island, as well as a comparison between the model results on waves and a simple theoretical 1D wave model. Chapter 5 will examine the model results with the island, and finally, chapter 6 will give conclusions along with some recommendations for future research.

2. BACKGROUND

This chapter will discuss relevant background information about what is known of the morpho- and hydrodynamics in the study area, as well as some theoretical background on waves that will be used later in this study.

2.1 STUDY AREA

The study area (included in Figure 4) is located near the Wadden Sea, which is registered in the UNESCO World Heritage List. More specifically, the eastern part of the Dutch Wadden Sea, roughly the area where the Dutch and German Wadden Sea meet. The Wadden system is a natural system of interconnected tidal basins with some relevant and important hydrodynamic and morphological characteristics that should be taken into account when studying the effects of artificial islands.

Furthermore, the Wadden region is part of the protected Natura 2000 areas. This is mainly due to the large number of birds that migrate to nest on the mudflats, salt marshes, and beaches and dunes. The birds are attracted by the abundant shellfish, worms, and other foods. The deeper waters are important for fish reproduction, and the Wadden Sea also accommodates seals (RHDHV, 2021). Since these areas are protected to preserve the nature and species that live there, rules are very strict with regards to construction works.

2.1.1 Geology and morphodynamics

The area of the Ems estuary (Figure 4) can be looked at as an example to give an illustration as to how dynamic the system is. A contributing factor to this is the so called 'erosion resistant layer'. This geological layer developed during the Pleistocene era and, because of its properties making flow and waves almost unable to erode the sediment, has a significant effect on the evolution of the seabed (WaterProof, 2022). Naturally, this has great influence on the protective layer of the cables, and therefore the routes along which these cables should be installed for optimal safety and efficiency. Other influences that can be thought of are dredging activities or the construction of hydraulic structures in the area.

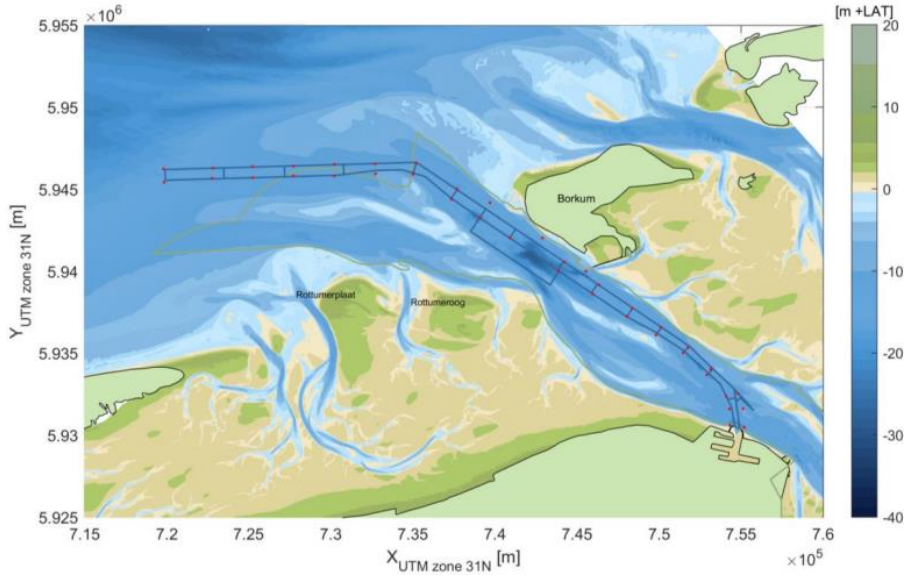

Figure 4 Bathymetry of the Ems estuary. (WaterProof, 2022) p.13.

There are several datasets/surveys available on the bathymetry evolution in the area, such as Vaklodingen, surveys from the Dutch Hydraulic Institute, and data from BSH. As can be seen from the ranges in Figure 5, the seabed in the area has fluctuated up to 10 m over the course of the last 40

years in certain areas. At some locations the range can exceed 10 m (WaterProof, 2022). These changes in the seabed level are caused by migration, aggradation and erosion of shoals, by channel deepening and migration, as well as scour holes and the presence of non-erodible layers.

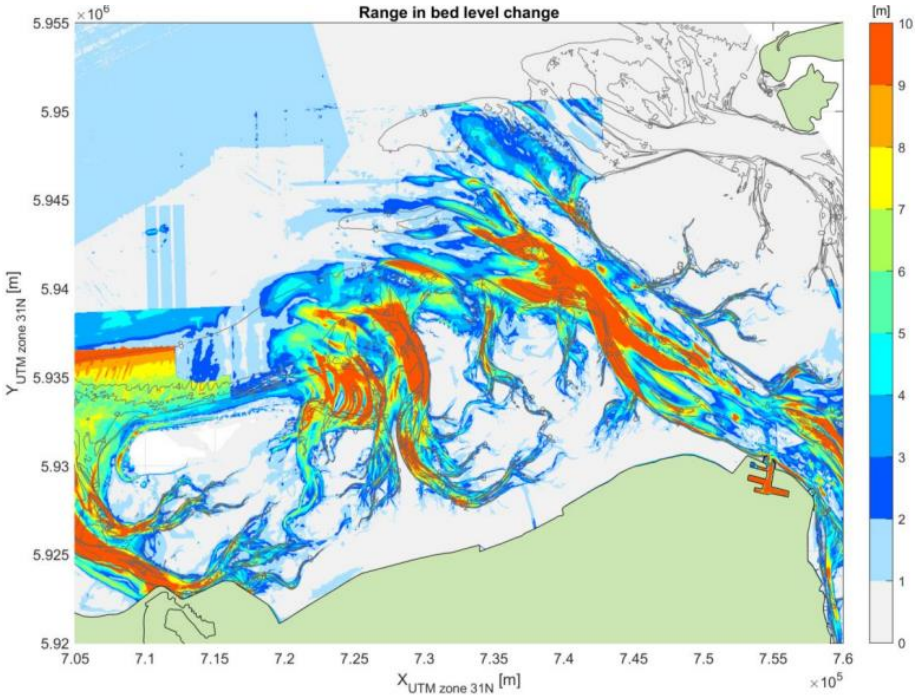

Figure 5 Bed level range between 1970 and 2020, (WaterProof, 2022) p.31.

2.1.2 Hydrodynamics

Aside from a dynamic morphology, the hydrodynamics in the Wadden Sea are also quite intricate. Water flows in and out of the Wad under the influence of the tides. Every 6 hours the direction of the current switches from west to east when the shallow Wadden system of channels and shoals is 'filling up', and when the same system is 'emptying out'. Since the tidal wave is coming from the west, high and low tide occur almost 5 hours earlier in Den Helder, at the west end of the Dutch Wadden Sea, than in Delfzijl, at the east end of the Dutch Wadden Sea, which is well-known from navigation (wadkanovaren.nl, 2021). On https://getij.rws.nl/ the high and low tide water levels and times can be found per tidal station employed by Rijkswaterstaat for recent years as well as for the year ahead. Though not all locations are available, an impression can be obtained by looking at a location that is close to the study area, like Schiermonnikoog and Huibertgat. High and low tide at Huibertgat can go up and down to a maximum of about 1.50 and -1.50 m NAP, respectively, a few times a year (Rijkswaterstaat, n.d.).

Currently, there is not really any direct measurement data available for the current velocities in the study area. Therefore, computational models are needed to predict these, which was done for this study.

Additionally, the area has its own wave characteristics. In addition to wind waves, swell waves are present at the North Sea side of the Wadden Islands and in the gaps between the islands. During storms, waves of as much as more than 7 meters have been measured offshore the North Sea coast of the Wadden Islands (Rijkswaterstaat, n.d.). In the Wadden Sea, also wind waves are present, which develop under the influence of wind on the wave energy and result in wave-induced currents (Grashorn, Lettmann, Wolff, Badewien, & Stanev, 2015).

2.2 WAVE THEORY

Within wave theory, the 4 main phenomena that will be examined in this study are shoaling, refraction, energy dissipation due to bottom friction, and wave breaking. The effects of which can be determined with linear wave theory for a simple bathymetry by computing the wave properties at each water depth. Recognizing these processes can help understand and model the hydrodynamics.

Starting with obtaining the wave length L [m] at each interval by iteratively solving the following formula:

$$L = L_0 \tanh\left(\frac{2\pi h}{L}\right) \quad (1)$$

Using the water depth h [m] and the wave length at deep water L_0, which can be obtained using the wave period T [s]. After finding L, the wave number k [m^{-1}] can be determined and used to find the wave celerity c [m/s]. Next, dimensionless variable n [-] (to obtain group celerity) can be found by solving:

$$n = \frac{1}{2}\left(1 + \frac{2kh}{\sinh(2kh)}\right) \quad (2)$$

And finally, the wave angle θ_w [deg] at each water depth can be found by using Snell's Law which states that $\frac{sin\theta}{c} = constant.$

After establishing these wave properties per water depth, the effects of shoaling bottom friction, refraction and wave breaking can be calculated.

2.2.1 Shoaling and refraction

Shoaling can be described as the "change in wave height due to effect of reduced water depth on group velocity" (van der Werf, 2021). This process is based on the assumption that wave energy (flux) is conserved, which means that the wave height will change when the water depth changes from deep to shallow. When no other are processes are present, the wave height will increase in shallow water closer to the shore due to shoaling.

Refraction can be described as the "change of wave direction in the nearshore due to the dependency of propagation velocity on the water depth" (van der Werf, 2021). Since waves are often not orientated directly normal to the coast, refraction will occur, which changes the direction of the wave towards shore-normal. This is caused by the decreasing water depth, which results in a decrease in wave propagation speed. The result is that the wave 'bends' towards the coast, which also has an influence on the wave height, though usually not as prominent as shoaling or bottom friction. The shoaling factor K_{sh} and refraction factor K_r are found by:

$$\frac{H}{H_0} = \underbrace{\sqrt{\frac{n_0 c_0}{nc}}}_{\text{shoaling}} \underbrace{\sqrt{\frac{\cos\theta_{w0}}{\cos\theta_w}}}_{\text{refraction}} = K_{sh} K_r \quad (3)$$

Where 0 stands for the deep water state. By multiplying these factors with the initial offshore wave height the effects of these processes on the wave height can be approximated separately.

2.2.2 Bottom friction

Next, bottom friction and wave breaking will induce energy dissipation. The shallower the water depth, the more prominent the effects of bottom friction are. The energy loss results in the lowering of the wave height as it nears the beach. To determine the effects of bottom friction, the change in wave energy should be established first. The total energy for a surface wave E_w [J/m^2] is the sum of the kinetic and potential energy and is described by:

$$E_w = \frac{1}{8}\rho_w g H^2 \quad (4)$$

This formula is used to find the initial wave energy density using the offshore wave height. After this, the energy loss due to bottom friction can be found by (van der Werf, 2021-2022):

$$D_{BF} = \frac{1}{T}\int_0^T \tau_b u_b dt = \frac{2}{3\pi}\rho f_w \hat{u}_b^3 \quad (5)$$

With dimensionless friction factor f_w and orbital velocity near the bed with angular frequency ω [s^{-1}]:

$$\hat{u}_b = \hat{u}(z=-h) = \frac{\frac{1}{2}H\omega}{\sinh(kh)} \quad (6)$$

To determine the new wave energy after dissipation, the energy flux balance is used. The energy flux [W/m] can be calculated by multiplying E_w with $c * n$ (resulting in the group celerity c_g [m/s]) and $cos\theta_w$. This term is included in the energy (flux) balance with a term accounting for the change in wave angle. This means that within this energy balance, shoaling and refraction are both incorporated as well. Together they should be equal to a source term that is negative in case of wave energy dissipation and positive in case of growth. The energy balance with dissipation will look as follows:

$$\frac{\partial}{\partial x}\left(E_w c_g cos\theta\right) = -D_w \quad (7)$$

After determining the energy loss due to bottom friction, the new wave height can be calculated based on the new wave energy. This is done by rewriting equation (7) and (4) respectively:

$$E_{w,x} = \frac{E_{w,x-1}c_{g,x-1}\cos\theta_{w,x-1} - D_{BF}\Delta x}{c_{g,x}\cos\theta_{w,x}} \quad (8)$$

$$H_{fric} = \sqrt{\frac{8E_{w,f}}{\rho_w g}} \quad (9)$$

Where Δx is the distance between two points on the bathymetry cross-section, set to a predetermined interval step size.

2.2.3 Wave breaking

Similar to bottom friction, wave breaking will cause energy losses notably in shallower water, but can also occur at deeper water depths. This energy loss is the result of the wave reaching a certain maximum steepness and breaking. There are 3 types of wave breaking: spilling breakers, plunging breakers, and surging collapsing breakers, which depend on beach slope, wave height, and period. Using Battjes' (1974) classification parameter, it is established that the type in this case is spilling breakers. The breaker parameter that is used for spilling breakers is $\gamma = 0.5 - 0.8$ (van der Werf, 2021). The following formula is used to approximate the wave height change in the breaker zone:

$$H(x) = \gamma h(x) \quad (10)$$

A rough approximation of the location of the breaker point can be found by combining this breaker model to the previous shoaling-refraction(-friction) model. This will be done by manually comparing the wave heights found by both models, and adopting the wave heights from the breaker model from the point where both models give (nearly) the same wave height or meet a certain condition (e.g. when the difference between the two is less than 0.01).

3. ISLAND DESIGNS

Islands can take on various forms and sizes. For this study, the island was not defined a priori, rather its design was part of the study itself. This section will discuss the procedure from design to implementation of the island(s).

3.1 DESIGNS AND SELECTION

Initially, various possible island shapes were created varying in shape and topology. Additionally, an island of a given shape and topology can vary in size and orientation. At a later stage, a selection was made to incorporate in the Delft3D model. In Figure 6, the following islands are shown:

- Shape 1 was added since it is the most simple island shape, it is a circular island with a certain radius that can be adjusted quite easily.
- Shape 2 is very similar to shape 1 with the addition of an L-shaped channel that leads to the interior of the island, which can accommodate a harbour.
- Shape 3 is a reproduction of the island shown in Liu et al. (2022). On the right side, a breakwater is present creating a bay in which the ships will be protected from possible harsh hydrodynamic conditions outside the bay.
- The fourth shape is quite similar to shape 3, but is inspired by the island design that was suggested during the early phase of this study.
- Shape 5 is a hexagon-shaped island, which resembles the circular shape 1, but being partially symmetric, hence with more possible variations in orientation.
- Shape 6, 7 and 8 are in essence quite similar to shape 5, with variations in the configuration by different number of sides for the discrete forms and the degree of smoothness of the island shape. These shapes were inspired by the “teardrop” shape recommendation from Lievense et al. (1994) that was followed in Deltares ((1999).
- Shape 9 was added as an alternative, simpler elongated shape, also with possible variations in the orientation.
- Shape 10 was inspired by conceptual designs of other energy islands, like in Denmark (State of Green, 2021), with a breakwater that is disconnected from the island.

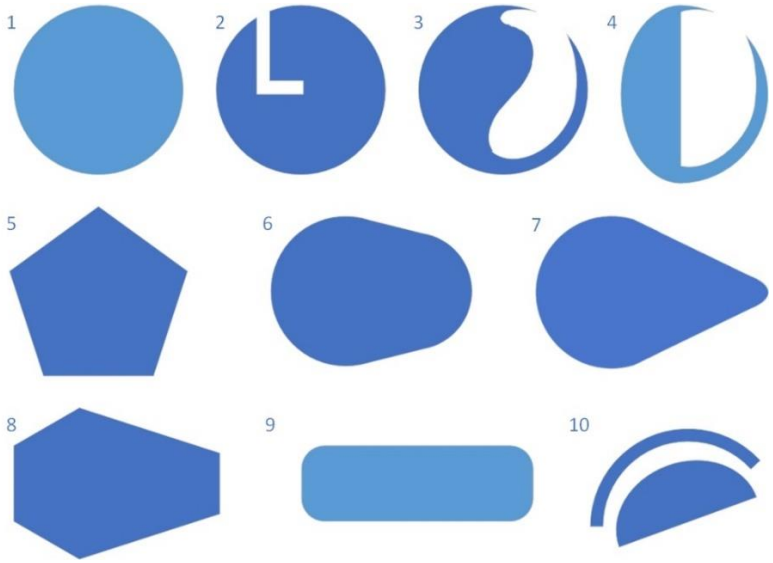

Figure 6 Island shape sketches.

After an initial discussion, 3 designs of the above-presented list were chosen to test with the model. These shapes are marked with lighter blue in Figure 6 (shape 1, 4 and 9). Shapes 1 and 9 were chosen

because of their simple shape, which renders the interpretation of effects when included in the model more straightforward compared to the more complex shapes, and taking into account the level of detail that is necessary at this stage of the overall study (i.e. conceptual design phase rather than detailed design). Shape 4 was selected considering how the design will likely look like at this stage, based on one of the earlier meetings with the client. The island will feature a breakwater/entrance in order to be accessible by ships. Later on, if needed, the more complex variations of the chosen designs (shapes 5, 6, 7, 8 as a variation to shape 1 or 9 and shape 2 and 3 as a variation to shape 4) can be added to the model. Though shape 10 would also be interesting to study, considering the level of detail and feasibility of the design (e.g. likelihood of the channel silting up), this design was left out as well.

3.2 ADDING DESIGNS TO THE MODEL

Once the desired configurations were determined, the shapes of the selected designs were recreated with python into an xyz-file with x- and y-coordinates of the outline of the islands, based around the coordinates of P1 and P6, and height z. It should be kept in mind that the depth is considered positive in the model, so the height in the script and xyz-files is set to -3 m (or -5 m). The slope is included by adding a so-called buffer of 150 or 15 m, which follows the contour of the shape, and setting the depth to 10 m below crest height of the island (+7 m in this case). Later, by interpolation in Delft3D QUICKIN, a slope of 1:15 or 1:1.5, respectively, will be reproduced.

After creating the xyz-files, they are loaded into Delft3D QUICKIN as samples. The result of the circular island will look like the left shape in Figure 7. Then, the grid that the model is based on should be loaded into QUICKIN (light blue grid in Figure 7), after which it is possible to make a depth file of the island by using *Triangular Interpolation* and saving the file. The resulting depth file can be seen in Figure 7 on the right. Once this file is saved, a new project should be started where the grid and original depth file of the model are loaded into QUICKIN first. Next, the previously created depth file of the island is imported as *Second Depth* and will be combined with the original depth file through *Change Depth to Min of Depth and Second Depth*. This means that the model will use the maximum height (= minimum depth) out of the 2 depth files. The result should be saved and can be used to run simulations with hydrodynamics, among others.

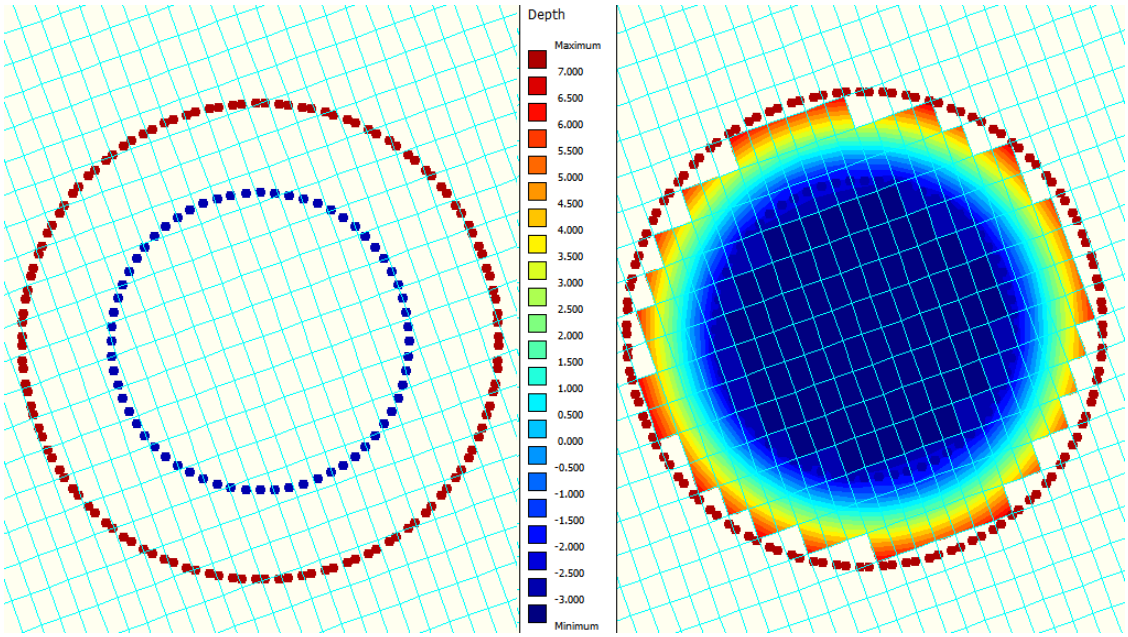

Figure 7 Left: Sample points of the round island outline with a buffer around it. Right: Result after triangular interpolation.

3.3 ISLAND SCENARIOS

After the selection of the 3 island shapes, several layout scenarios were outlined based on the island design parameters shown in Table 1, with options per category. In addition, extra features like dams, breakwaters and an entrance channel are also possible options. The categories that are listed are briefly elaborated below. The most interesting combinations between these categories were simulated. An overview of the simulated cases is listed in Table 3 in chapter 5. An overview of other possible island parameter combinations is shown in Table 4 in appendix A.

Table 1 Design parameters

Location	Size	Shape	Orientation	Height	Slope
A. P1	A. Order of 50 m	A. Round	A. E-W (east west)	A. 3 m NAP	A. 1:15
B. P6	B. Order of 500 m	B. Elongated	B. N-S (north south)	B. 5 m NAP	B. 1:1.5
		C. Half ellipse (with breakwater)			C. Combination 1:1.5 & 1:6
		D. Ellipse			

Location

The location of the island is based on the options that were defined from a previous study (P1-P4 from west to east). Two additional locations were added east of the previously determined positions. The locations that were chosen to simulate with initially are the most western location and the most eastern location, as shown in Figure 8. After the first simulations with the round island variants, it was opted to simulate the rest of the scenarios for location P6 only, to minimise the number of simulations since it seemed more interesting from the initial results. During a later meeting with the client, P6 also emerged as the preferred location for the island.

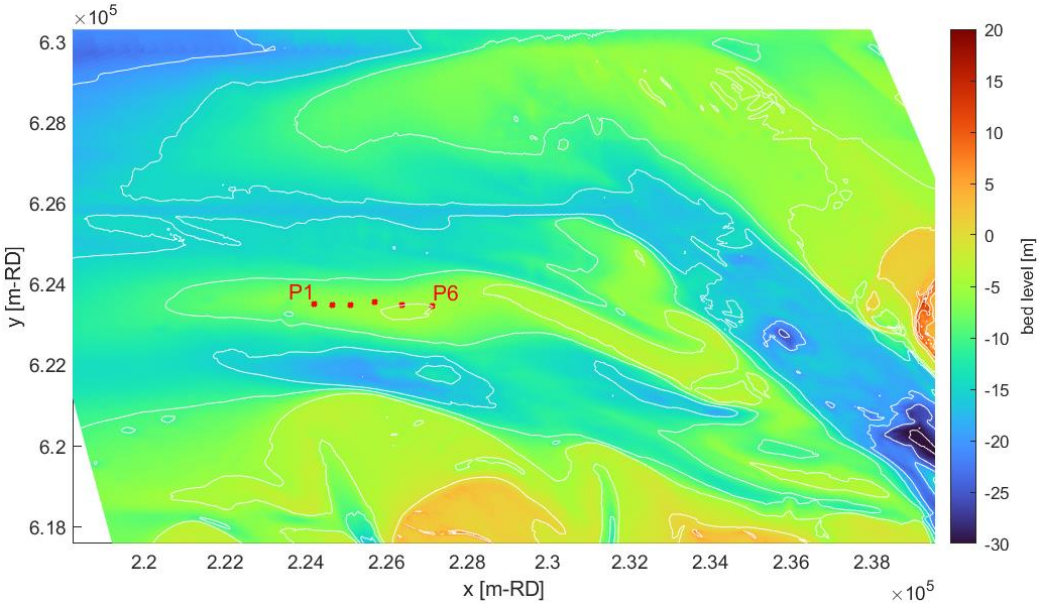

Figure 8 Possible island locations on the Ballonplaat.

Size

The size of the island is an important factor as it has an influence on the effects on the hydro- and morphodynamics. Two sizes were selected: a relatively small island (order of 50 m) and a relatively large island (order of 500 m). The 500 m case was proposed during an initial meeting with the client, and is based on the space that is expected to be needed to accommodate the tunnel entrance/exit

on the island. The smaller case was defined in order to be able to contrast the effects to that of the larger island.

Shape

The shape parameter relates to the shapes chosen in the previous section. An additional ellipse shape was later included following the second meeting.

Orientation

The orientation is important for shapes except the circular shape. The angles were set to either 15 degrees or 285 degrees with respect to the North, which is approximately parallel or transverse to the flood/ebb flow direction based on the first simulations of the current situation without an island.

Height

The crest height of the island was set at 3 m NAP so that water cannot flow over the island. In a following meeting, a new crest height was proposed of 5 m NAP to ensure that the island stayed dry. This was, however, not incorporated in the models studied for this thesis yet.

Slope

An initial slope was defined at 1:15 to soften the island edges and to create a more gradual transition between the island and the area around it. In a next meeting, it was discussed that this slope will likely be constructed at a steeper angle (1:1.5).

4. RESULTS WITHOUT ISLAND

The modelling software that is used in this study is Delft3D(-FLOW). Delft3D is a hydro- and morphodynamic simulation program developed by Deltares and was coupled to a SWAN wave model. The software is used to conduct simulations of currents, waves, water quality, and ecology in coastal, river, and estuarine areas. Additionally, Delft3D is used to compute sediment transport and morphological developments in these areas. It consists of several modules that are grouped around a mutual interface and can interact with one another. As the name suggests, it can perform simulations up to 3D and calculates on a rectilinear or a curvilinear, boundary fitted grid. (Deltares, 2022) In this study, a boundary-fitted structured grid is used for the area near the eastern Dutch Wadden Sea and Ems estuary.

4.1 MODEL STRUCTURE AND ASSUMPTIONS

Structure and settings

The boundary-fitted structured grid of the study area has a size of 653 by 542 cells and is slightly rotated at an ~20 degree angle. The model is nested in a bigger model of the whole Ems, which is nested in an even bigger model of the Eastern Wadden Sea, which is nested in a model of the Dutch coast, which is nested in an even bigger model. The boundary conditions of the current model are obtained from the bigger model(s) and used as input.

At the edges of the model, boundary conditions are defined for boundary segments which can be open or closed. In Figure 9, an overview of the modelled study area in Delft3D can be seen, where the blue-coloured lines indicate the location of the open boundaries of the model. At these boundary segments, the current conditions are defined as well as the Riemann type of boundary conditions are prescribed. Riemann conditions are a combination of water level and currents, and are prescribed as time-series. At the border locations in Figure 9 where no blue line is visible, the boundary is closed, implying that the current velocities normal to these boundary segments are set to zero (no flow across the boundary).

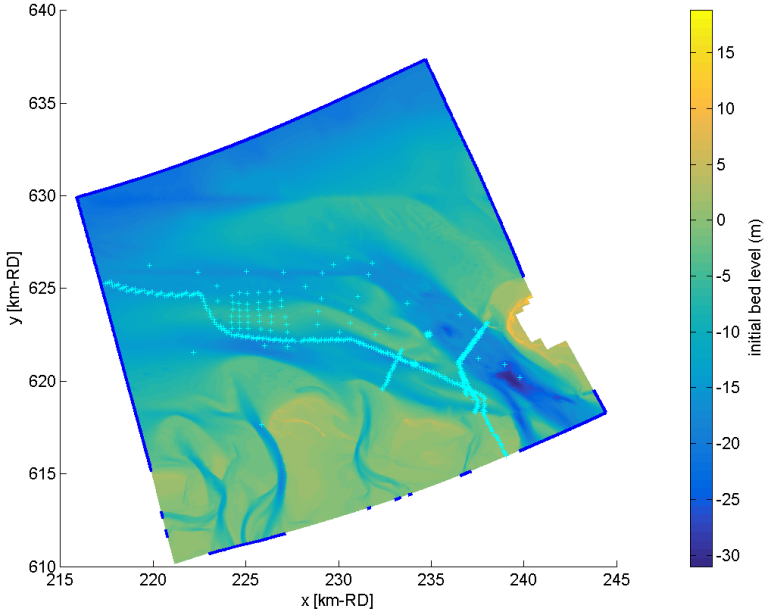

Figure 9 Overview of the model area as in Delft3D. Monitoring points for which high time-resolution output data are available, are shown as cyan-coloured points.

The model monitoring is set from 20-06-2022 00:00:00 until 23-06-2022 00:00:00 (forming part of a period during which measurements were conducted in the Ems area), but the simulation started

earlier and ran from 01-06-2022 until 01-07-2022. This is done to allow for the model to start up gradually and realistically mimic the current situation. The results were stored with output time intervals of 10 minutes for both the entire model grid and at specific monitoring points (cyan-coloured points in Figure 9).

Assumptions

Some assumptions and choices that are made in the model are:

- Depth-averaged assumption (2-D), so no variations over the water column are considered,
- Constant salinity,
- Uniform roughness of 0.01 (White-Colebrook) and uniform horizontal viscosity of 1 m2/s,
- Waves are based on the JONSWAP spectrum,
- Wind effects are not included

4.2 CURRENT HYDRODYNAMICS (WITHOUT ISLAND)

Model simulations were done with low, year-round waves of 1 m significant wave height (Hs) and a peak wave period of 6 s, and high storm waves of 7 m Hs with a peak wave period of 13 s.

4.2.1 Significant wave height

Figure 10 shows a map of the resulting significant wave heights at a certain timestep on June 20th for the year-round (left) and storm (right) wave conditions. From the results shown in the figure, it can be seen that the waves are highest at the north/north-west side of the model, which is where the bed is the lowest, thus where the water depth is the greatest. This makes sense, because the greater water depth allows for greater wave heights without the restriction of the bed. In the year-round wave model the waves seem to become lower towards the south rather gradually from 1 m offshore to around 0.8 m near P6, while for the storm wave model the significant wave height quite abruptly basically halves from 7 m to about 3 m. This can be explained by the presence of a shoal called the Geldsackplatte. From the top view on the right of Figure 10, it can be seen that the sudden decrease in significant wave height follows the contours of the shoal. This clearly shows the impact of the water depth on the wave height. Other than that, the overall pattern of the waves appears quite stable with some variation in time for both cases, which points at tidal modulation of the wave height due to changes in water depth.

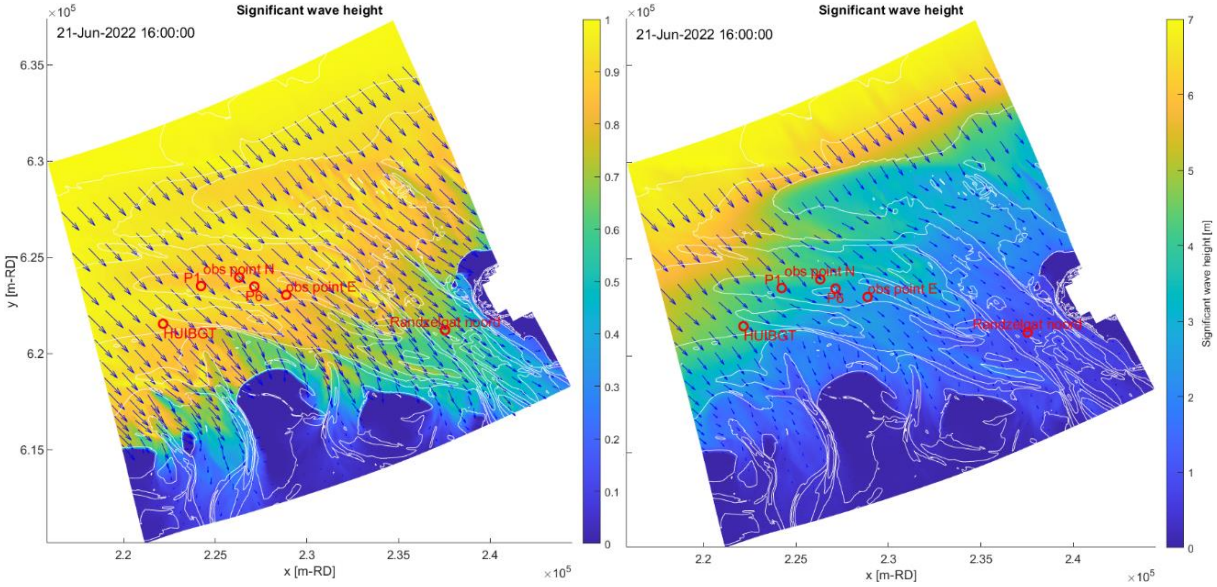

Figure 10 Significant wave height results for year-round waves of 1 m (left) and storm waves of 7 m (right) during flood tide. Note the difference in range between both colorbars.

4.2.2 Depth-averaged velocity

An overview of the computed depth-averaged velocity over the whole grid is depicted in Figure 11, for the situation with simulated year-round waves on the left and storm waves on the right. Both snapshots are on 20/06/2022 at 18:20:00, which is roughly at peak ebb velocities of observation points N and E and Randzelgat Noord as shown in the timeseries plots (see inset). From the maps, it can be seen that overall high current velocities (up to almost 2 m/s) occur in the channels which discharge most of the tidal water volumes.

In general, the same pattern appears for both the low and storm waves. Where in the storm wave case higher velocities appear until farther up north in the channel. The increased velocities in the channels are an addition of the tidal currents and the currents that are induced by breaking waves. The latter causes mass transport of water, which generates currents that add to the currents that were already present.

At certain depth contours, such as that of the Ballonplaat (see zoom inset in Figure 11 on the right), the velocities decrease rather abruptly and locally even form vortex-like shapes as can be seen at the top of the right figure. This is caused by the relative shallow water depth compared to the wave height, which, due to the interactions with the tides, induces flow circulations. Also at the northern edge of the Ballonplaat horizontal cell circulations are caused by the change in water depth. At the possible future island location P6 the velocities reach around 0.6 – 0.8 m/s for the year-round wave and 0.4 – 0.8 m/s for the storm wave, both at high tide.

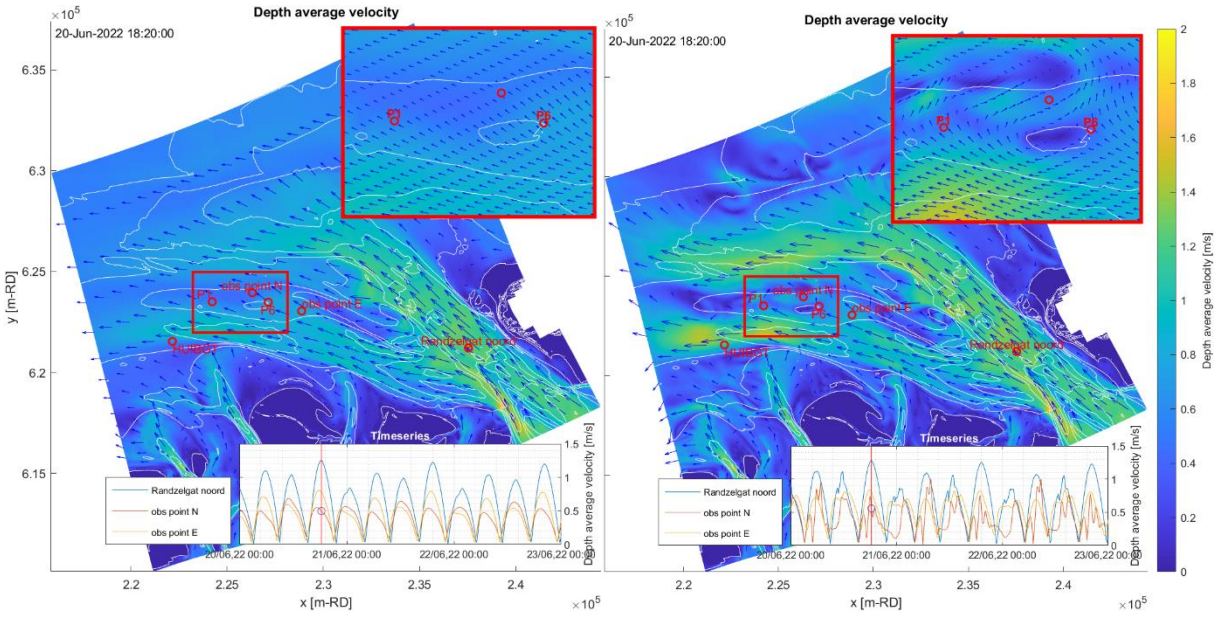

Figure 11 Depth-averaged velocity results with year-round waves of 1 m (left) and storm waves of 7 m (right) on 20-06-2022 18:20:00 during ebb tide.

In Figure 12, the computed currents during flood tide are shown on 21/06/2022 at 14:20:00. At this timestamp, an interesting situation occurs where the overall depth-averaged velocity pattern for low and storm waves is reversed. Looking at the results with low waves, a similar pattern as discussed previously can be seen where the depth-averaged velocity over the Ballonplaat is a bit lower than around it in the channels. However, with storm waves the velocities directly over the Ballonplaat reach speeds of about 1.5 m/s, whereas the velocity directly outside of the shoal's contour drops to locally nearing zero. This is as expected since the waves break on top of the Ballonplaat, thereby generating strong currents.

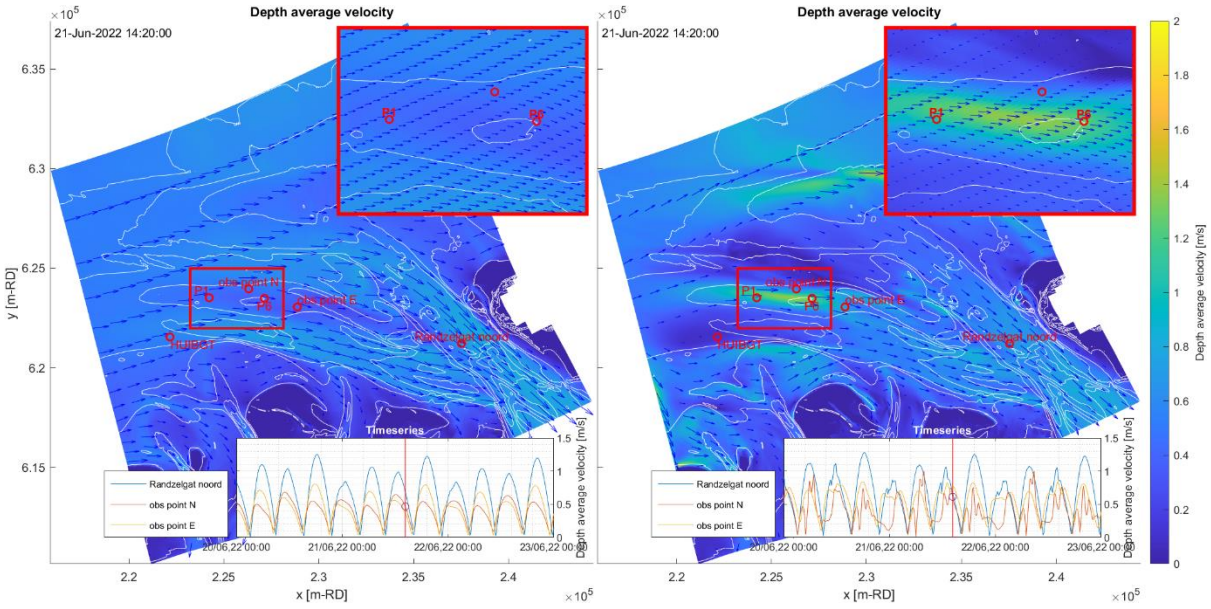

Figure 12 Depth-averaged velocity results with year-round waves of 1 m (left) and storm waves of 7 m (right) on 21-06-2022 14:20:00

4.3 MODEL VS THEORY / SWAN VS 1D THEORETICAL WAVE MODELS

In this section a comparison is made between the results of the 2D SWAN model and a theoretical 1D method to see how the results differ, and whether the use of a 1D method would also suffice for this analysis. To this end, three cross-sections have been defined, all beginning at a distance of 8000 m at an angle of 0 (1) , 270 (2) and 315 (3) degrees from N, and ending at the P6 location. Cross-sections 1 and 3 are chosen as directly coming from the north and west of the island and cross-section 2 approximately running parallel to the wave direction. See Figure 13.

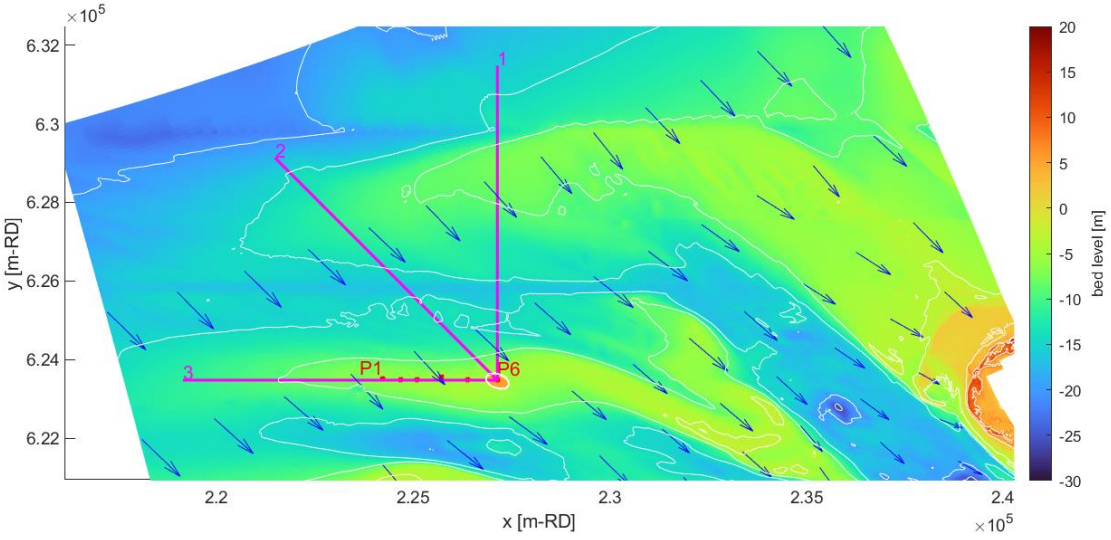

Figure 13 Overview of the cross-section locations with wave direction arrows

4.3.1 Theoretical 1D wave model method

Three theoretical models were built in Excel, each applying the effects of shoaling, bottom friction, refraction and wave breaking in a different way. The first Excel model closely follows the method and order of the theory as explained in section 2.2, which was based on van der Werf (2021). The input variables of the models are shown in Table 2. Two other Excel models were developed by van Rijn (van Rijn, 2011).

Table 2 1D wave model descriptions

Model	Principle	Input	Program
1	Using linear wave theory with energy balance and manual breaking (as explained in chapter 2.2) based on van der Werf (2021)	Offshore: wave height, period, angle; distance from offshore; water depth; breaker parameter; friction factor; number of steps;	Excel / Matlab
2	Simple linear wave theory (coefficients for shoaling, refraction and friction as: Hs = Ks*Kr*Kf*H0) developed by van Rijn	Offshore: wave height, angle, period; breaker coefficient; friction factor; distance from offshore; water depth	Excel
3	Implementation of Battjes-Janssen (1978) developed by van Rijn	Offshore: wave height, angle, period; breaker coefficient; bottom roughness; grid size; water depth	Excel

Model 1

After entering the input variables mentioned in the table above, the first Excel model calculates the wave length at each water depth. Initially, the *Solver* function in Excel was used to compute this with equation (1), but this only worked well for bigger grid/step sizes (less variables). Later, the wave lengths were calculated using Matlab (*fzero*, which accomplishes the same as *Excel Solver* but faster) and copied into the Excel model to save time. After this, all parameters for shoaling and refraction are computed for each water depth in a column wise manner (top to bottom, left to right). Technically, shoaling and refraction are already incorporated in the method for calculating bottom friction, but are calculated separately to be able to see the contribution of each process.

For bottom friction (including shoaling and refraction), the energy balance is used and the wave height of the previous step is needed to calculate the new wave height. This means that the essential parameters (D_{bf}, E_w, H_f) are computed from left to right at each step (left to right, top to bottom). Finally, wave breaking will be manually applied by comparing the resulting wave heights obtained after applying shoaling, refraction, and bottom friction to the wave heights computed with the breaker formula (equation (10)). If the difference between these wave heights reaches under the threshold of 0.01, the wave heights obtained at that water depth will be replaced by the wave heights found with the breaker formula. A Matlab model was constructed which basically operates in the same manner but is used as a check for the Excel model.

Model 2

The first, simpler model by van Rijn (Model 2) is similar to the previous Excel model and also calculates column-wise from top to bottom, left to right. However, to determine the wave height, it uses coefficients for shoaling, refraction, and also for friction. In addition, the model includes (average) wave setup in the surf zone, which affects the water depth in that region, and therefore the wave height. In this model, breaking is also “manually” added when the calculated wave height is smaller than the wave height found by the breaker formula.

Model 3

The second model by van Rijn is based on the model description by Battjes and Janssen (1978) (Model 3). It generally uses a similar approach to the model based on van der Werf (2021), where it computes the wave heights based on the energy balance. However, this model incorporates breaking as a factor/coefficient which is applied to all wave heights (not only when a condition is met).

4.3.2 Comparison results

The models were compared for 3 cases: using a linear bathymetry (Figure 14), using the real bed profile as obtained from the SWAN model (Figure 16), and using the real profile with the added island (Figure 25 in section 5.5). Additionally wave 2 scenarios were compared: the year-round waves

(1 m) and storm waves (7 m). The comparison results with island will be discussed later in chapter 5.5.

Theoretical profile

The theoretical bed profile was set to a water depth of 0 – 25 m and a distance of 3000 m, resulting in a slope of 1:120. The resulting wave height development for the 3 models is shown in Figure 14 below.

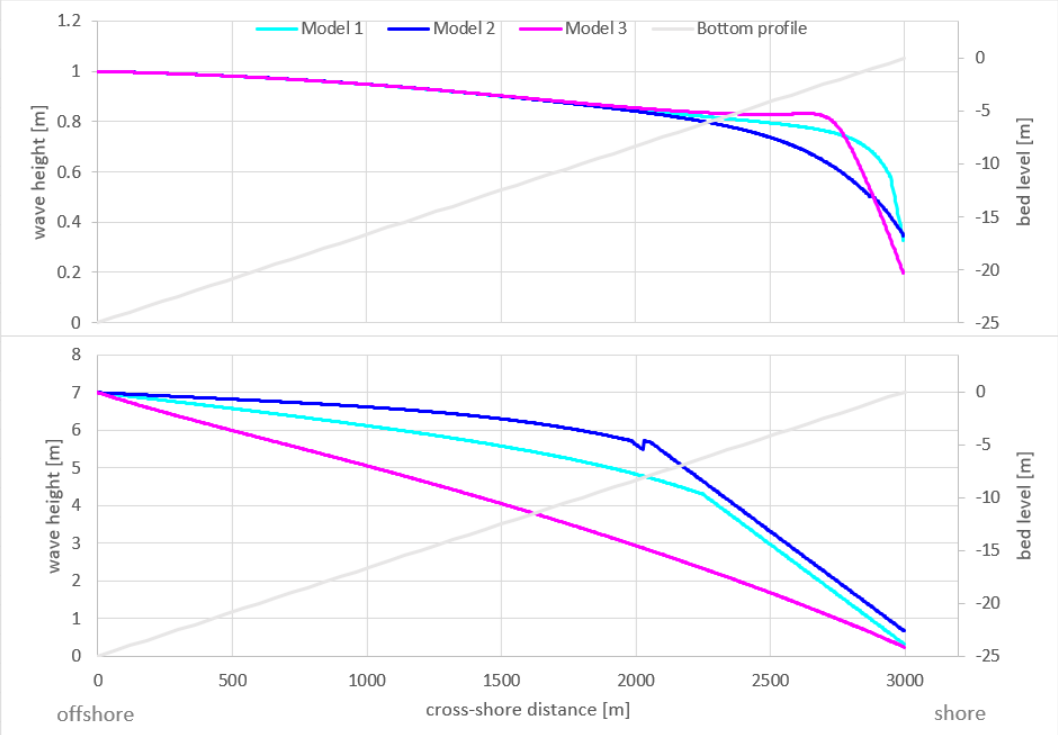

Figure 14 Results 1D wave models for a linear bathymetry with year-round waves (top), and storm waves (bottom)

Year-round wave conditions

On a linear bed profile, the wave height will decrease due to the effects of bottom friction, refraction and wave breaking, and will, in case a trench is present, increase due to shoaling. The top plot of Figure 14 shows that all models compute the same wave height up to a water depth of approximately 10 m at a cross-shore distance of around 1700 m. This validates the basic implementation of the models, as they all seem to give the same result for a simple linear profile in relatively deep water.

Taking a closer look at the differences between the resulting wave heights of the models in Figure 15, it can be seen that Model 1 computes a very slow decrease until a depth of about 1.5 m. Here, the effects of bottom friction start to become more important until the waves break at a depth of less than 1 m.

Next to that, it can be seen that the first model by van Rijn computes relatively lower wave heights, with the shallow decline representing a gradual decrease of the wave height. The decrease in wave height earlier offshore, compared to the other models, can be explained by the dominance of bottom friction in this model. Because of this, the effects of wave breaking are also less extreme compared to the other two models.

In contrast, the second model by van Rijn computes higher wave heights, even showing a slight increase in wave height before it decreases. This shows that the effect of shoaling is more prominent

in Model 3, causing more intense effects of wave breaking closer to the shore which can be seen at around a depth of 2 m. Here, the wave height decreases at quite a steep angle because bottom friction becomes more prominent due to the relatively large wave height compared to the water depth.

More concrete, the differences in wave height between the models can be mainly explained by different ways in which the effects of bottom friction are modelled. Due to lack of time, and this particular subject not being the main focus of this thesis, these differences cannot be dealt with in more detail, but could form a starting point for a future research.

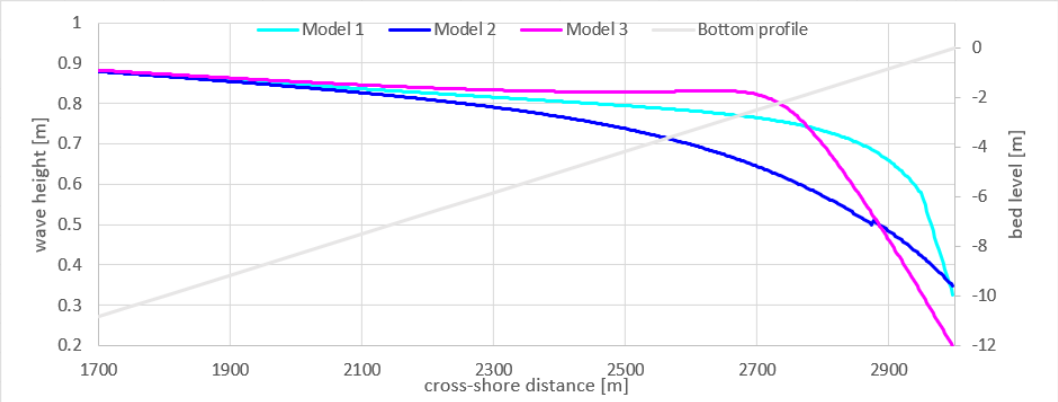

Figure 15 Zoom of the year-round waves on a theoretical profile

Storm wave conditions

When looking at the results for the storm wave (bottom plot in Figure 14), the predictions of Model 1 seem to be right in the middle of the models by van Rijn. Model 3 almost has a linear development of the wave height, following roughly the inverse of the bed profile. This is likely due to the effects of bottom friction already becoming dominant because of the wave height being large compared to the water depth. Model 1 and 2 appear to be following the same slope closer to the shore because of the similar implementation of wave breaking. The difference in wave height from around cross-shore distance 2300 m can be explained by the fact that Model 2 also includes wave set-up.

At first glance, the relative plot position of the 2 models by van Rijn seem to have been swapped. However, when taking a closer look, the order in wave height at the shore is the same. Bottom friction had a very gradual effect for the first model by van Rijn. The same can be said when looking at the curve for the storm wave.

The second model by van Rijn (Model 3), however, was quite sensitive for bottom friction once the water depth became relatively shallow. In comparison, where the model started showing a steep change the ratio between water depth and wave height was about 0.3, while this ratio for the storm wave is already almost 0.3 at the offshore. This means that bottom friction will be very prominent in the results for this model throughout the entire cross-section.

Realistic seabed profile without island

The realistic seabed profile was determined through Delft3D for the cross-sections as shown in Figure 13. The cross-shore distance of the sections is 8000 m with the bathymetry varying between 5 and 18 m water depth. The results shown in this section are for cross-section 1, extending from the north of location P6, corresponding to general wave angles of 45 degN relative to coast normal.

The results of the models are shown in Figure 16. The first thing that stands out is that the offshore wave height of the 1D wave models is different from the SWAN model. This is because the offshore

wave height in SWAN starts further offshore at greater water depth, thus the wave height has already decreased by the time it reaches the location where the cross-section starts.

In the offshore area all models show roughly the same pattern after the first small bump in the bathymetry at around 1800 m, including the SWAN model. This changes when a big 'bump' appears, which is the Geldsackplatte, also visible in Figure 13 as the green area that line 1 crosses. There, the model results start to diverge up to about 0.1 m, with the first van Rijn model computing slightly higher overall wave heights compared to the other models. This could be explained by the fact that it is a very simple method, while SWAN and Model 3 include a lot more variables, parameters, and in the case of SWAN, inputs.

With this logic, the low result of Model 1 seems a bit unexpected but could be due to an overestimation of the effects of shoaling, bottom friction and refraction. However, the shape of the wave height development does resemble Model 3. This is also the case for Model 2, until towards the end where friction starts to play a big role in the model and causes a strong decrease in wave height resulting in lower predictions than all other models, deviating around 0.2 m from the SWAN model results. Another surprising observation is the sudden increase in wave height in the SWAN model, considering the decreasing water depth. A possible explanation for this is the occurrence of convergence of the waves, which causes larger wave heights.

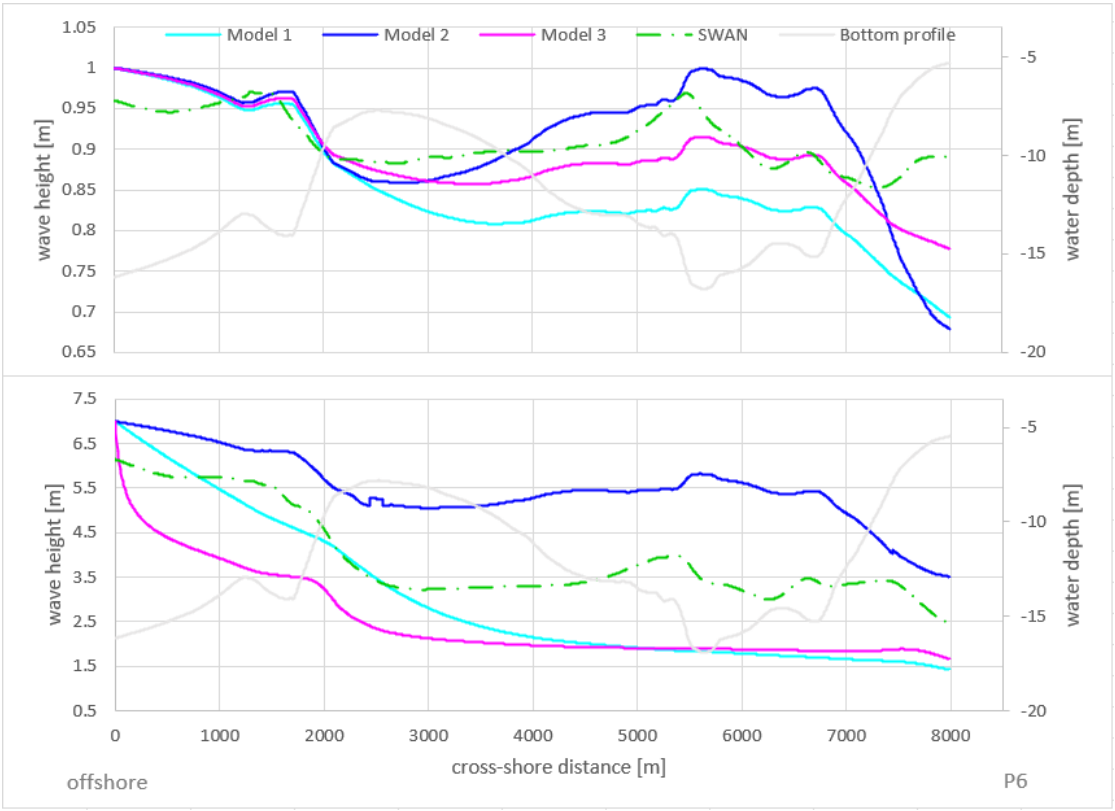

Figure 16 Results of the 1D wave models and SWAN for the real bathymetry without island with year-round waves (top), and storm waves (bottom)

Now looking at the results for the offshore storm waves, the wave heights deviate quite a lot from each other, up to 2 m throughout the cross-section, but up to 0.1 m close to the P6 location. This is to be expected, especially when comparing a 1D model to a 2D model. Once again, the first model by van Rijn (Model 2) computes higher wave heights (or smaller effects of shoaling, refraction, bottom friction, and wave breaking), for the entire cross-section. The second model by van Rijn (Model 3) shows a strong decrease in wave height early on at the offshore region, which reduces for a bit after

the first small 'bump' in the bathymetry. After the Geldsackplatte the wave heights obtained through Model 3 and Model 1 start to appear more similar until it reaches the end of the cross-section. The result from SWAN lies somewhere in between the aforementioned models and Model 2. Interestingly, while the bottom profile still roughly reappears in the wave height development of both Model 2 and SWAN, this does not happen for Model 1 and 3. An explanation for this cannot be given currently, but would be interesting to investigate further.

Effects wave angle

Another varying factor that is interesting to look at is the effect of the initial wave angle in relation to the shore-normal. Excluding the differences in bathymetry, the wave angle is most influential for wave height changes due to refraction. However, as this is a real bathymetry, the cross-sections that are at differing angles, also have varying profiles, which are depicted in the top of Figure 17. Cross-section 3 stands out because of its linear shape. This cross-section is located west from P6 and stretched over the Ballonplaat. Looking at the results for this cross-section gives a comparison between a true theoretical (straight) profile and a real approximation of a theoretical profile. Since the offshore bed level in the theoretical example was lower, the ratio between wave height and water depth in smaller for the real bathymetry. Hence, the result for the year-round wave looks like the result for the storm wave in Figure 14.

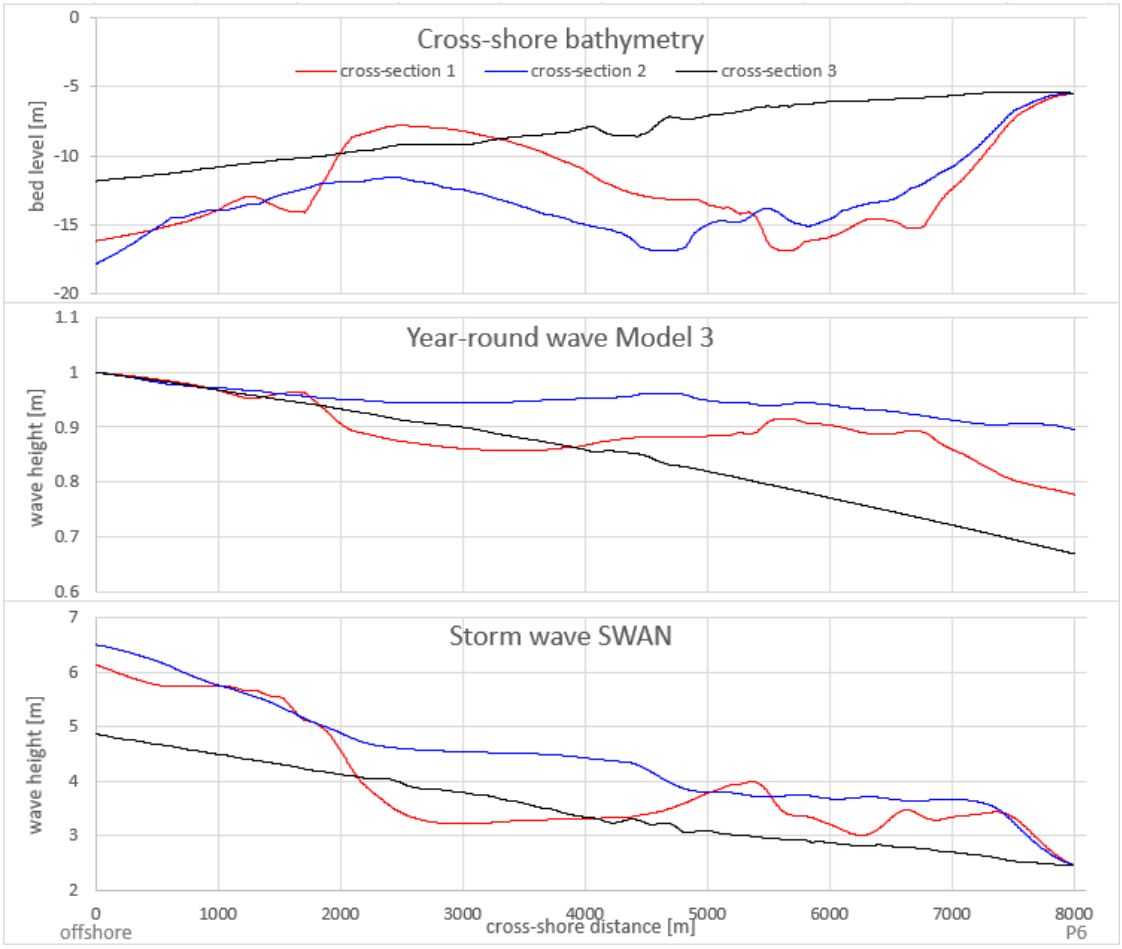

Figure 17 Results for varying initial shore-normal wave angle. Top: bed level, middle: results year-round wave for Model 3, bottom: results storm wave for SWAN model

4.3.3 Discussion

As can be seen, the different models give somewhat varying results depending on how the model is set up and what the main purpose of the model is. In addition, assumptions can differ from model to model. By tuning these, results can start to resemble or differ from each other more.

A big assumption that is being made when comparing the SWAN model to the 1D model is that linear wave theory is applicable, which is what the models are based on. The applicability of linear wave theory can be determined using the Ursell parameter, defined by (van der Werf, 2021):

$$Ur = \frac{HL^2}{h^3} \qquad (11)$$

For which $Ur < 15$ linear wave theory is applicable. For the year-round wave this condition is met until the water depth reaches a bit under 4 m (for cross-section 1, for the other cross-sections a bit earlier). For storm waves non-linear wave theory actually turns out to be more reliable, showing values much higher than 15 for Ur. This means that in the case of storm waves, the validity of the 1D models can be questioned and the results should be interpreted with caution.

Next to this, dimensionless parameters that are part of the theory are set to an assumed value, which was not necessarily based on the natural conditions in the study area. The friction factor f_w is such a parameter. In Model 1 and Model 2 a value of 0.075 was assumed, but adjusting this number can affect the result of the models quite significantly.

Another factor that can affect the results and how they appear, is the grid size/resolution. A notable example is the energy dissipation, that is calculated per running meter or a set distance. Some problems arose when setting the grid size to 100 m, so it was changed to order 10 later to decrease the step size. Setting this distance too large can cause weird jumps in results, making the results unreliable. Moreover, in terms of plotting the results, a resolution that is too low can also hide important details that could be important.

Finally, another factor that should be taken into account is that the 1D models do not take time into account (and other relevant factors), while for showing the SWAN results a timestep should be selected. Though, no huge variations in time are visible (no island case).

5. RESULTS WITH ISLAND

The general settings and assumptions for the simulations with island are the same as for the case without island, as described in chapter 4. All 4 configurations in Table 3 are simulated without waves, to focus on how the depth-averaged velocity is affected. In addition, the large half ellipse island shapes with both orientation scenarios are simulated once more with waves to determine the possible effect on the depth-averaged velocity as well as the effect of an island on the significant wave height. In total 6 island cases are simulated to show what the changes are in wave height or flow patterns due to the island according to the SWAN model. An overview of the simulated island configurations is shown in the table below.

Table 3 Simulated island scenarios

Simulation ID	Location	Size	Shape	Orientation	Height	Slope
003d	P6	Order of 50 m	Circular	-	+3 m NAP	1:15
003e	P6	Order of 500 m	Circular	-	+3 m NAP	1:15
003f/303w	P6	Order of 500 m	Half ellipse	N-S	+3 m NAP	1:15
003h/305w	P6	Order of 500 m	Half ellipse	E-W	+3 m NAP	1:15

5.1 EFFECT OF ISLAND SIZE

To illustrate the significance of the size of an island on the hydrodynamics in the area, a small and large circular island shape are simulated of order 50 m and 500 m in diameter, respectively. At this stage, no waves are included yet. A snapshot of the resulting depth-averaged velocities is shown in Figure 18.

5.1.1 Small circular island

The first case was simulated to get a picture of the effects of a small island of dimensions 50x50 m. As mentioned before, this is not a realistic size for a workable island for its purpose but was simulated to contrast with an island of bigger dimensions. The resulting depth-averaged velocities are shown in the top plot of Figure 18. Quite surprisingly, the small island already had quite a big impact on the depth-averaged velocity. From the plot, shading resembling a vortex street starts to appear behind the island (relative to the flow direction), where the darker colour indicates that the velocities in that area are decreasing. This already happens for the small island case reaching approximately 1 km in stretch at first glance, but reaching even further up to nearly 4 km at times when inspecting the results at closer detail.

To explain a bit more about the vortex street (also called Kármán vortex street), vortex shedding should be discussed, which is the process that causes the vortex street to appear. Vortex shedding occurs in liquids as well as in gases, when the fluid passes a cylinder or other bluff body. The flow will split and periodically shed vortices from the body surface. This only happens under specific conditions, such as a certain range of velocities and the size and shape of the body. The frequency at which the vortex shedding occurs is related to the Strouhal Number, which also depends on the Reynolds number.

Informally, the pattern appears because the water gets deflected to both sides of the island. The flow “sticks” to the island in the boundary layer, which makes the streams on either side bend towards each other again. Because these streams are not exactly of equal magnitude, they create a zigzag

pattern behind the island. Close to the island, where the water gets deflected to either side of the island, the velocities increase somewhat, and also slightly increase along the lee side of the island (with respect to the tidal flow direction).

5.1.2 Large circular island

Compared to the smaller island, other than the area covered by the island (where u = 0), the shape of the darker area in the bottom plot of Figure 18 is quite different. When zooming in on the island a distinct wake can be seen, which later turns into a pattern. However, where the small island induced a clear zigzag pattern, the large island creates more of a swirl. When looking at the animation of the whole map, the darker area further downstream of the island begins to show the start of a zigzag. However, because of its size it does not seem to have enough space to develop into a zigzag with multiple oscillations. This space is determined by the bathymetry in the area, which is relatively small comparing the diameter of the island to the width of the Ballonplaat. Because the water gets deflected over a larger area, the higher velocities at the flanks of the island (relative to flow) cover a larger area than for the small island case. The increased velocities also follow the contour of the darker area behind the island for a longer distance because of the difference in size. This creates similar velocities over the Ballonplaat, at the level of the island, as in the deeper fairways north and south of it.

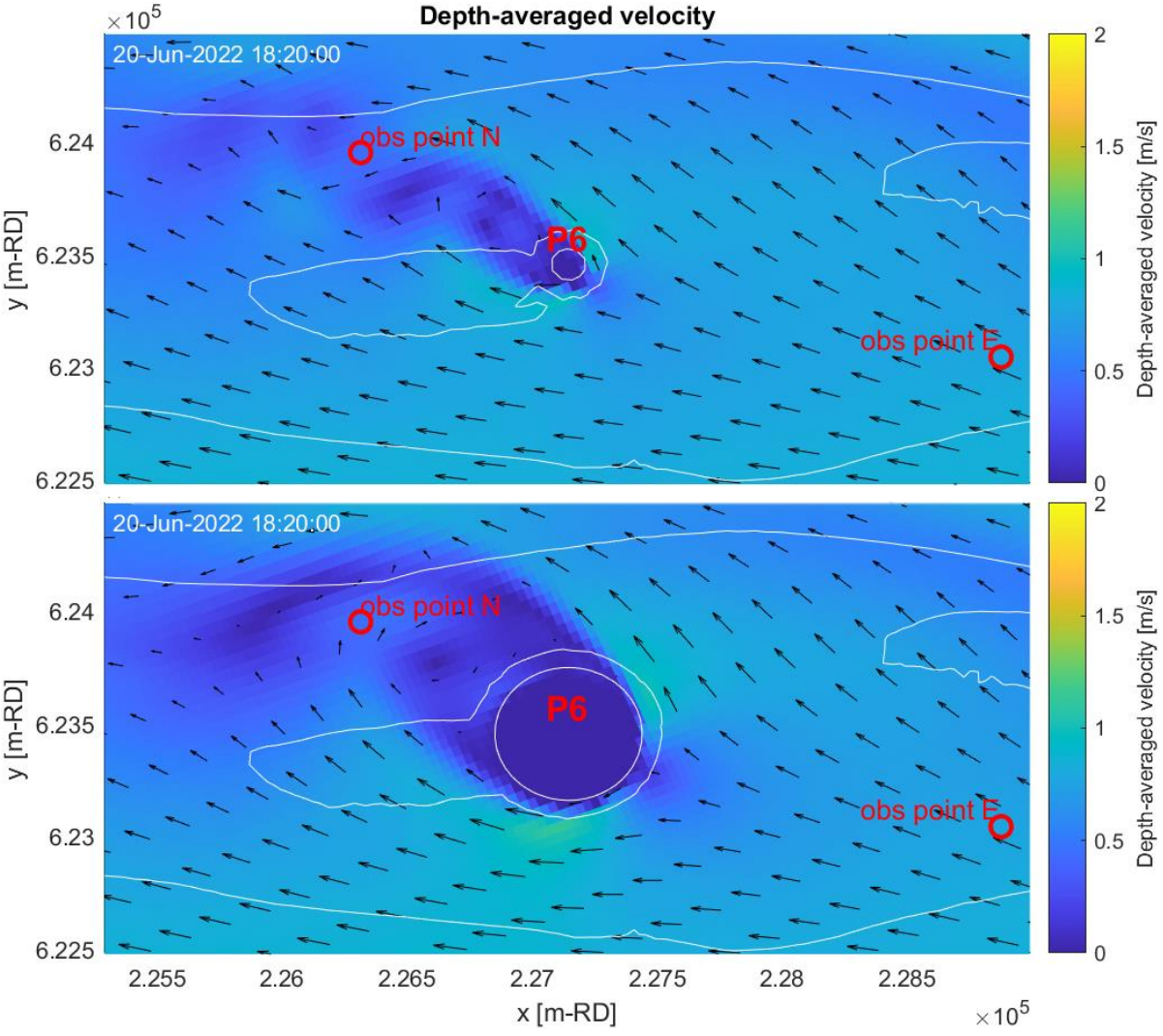

Figure 18 Depth average velocity results for the small circular island with d = 50 m (top) and large circular island with d = 500 m (bottom).

5.2 EFFECT OF ISLAND SHAPE & ORIENTATION

Aside from the size of the island, the orientation of a non-circular island can also greatly influence the hydrodynamics in the area. To show this, a comparison is made between a “favourable” orientation, approximately parallel to the flow direction and aligned with the Ballonplaat, and an “unfavourable” orientation, perpendicular to the flow direction and the orientation of the shoal. The island shape that is used for this is the large half ellipse shaped island with the straight quay facing the east (N-S orientation, so considered unfavourable) or the south (E-W orientation, considered favourable), as shown in Figure 19 and Figure 20, respectively. In this analysis waves are still not added yet.

5.2.1 N-S orientated large half ellipse shaped island

When looking at the resulting depth-averaged velocity plot in Figure 19, it is immediately noticeable that the shape of the wake area is quite different from the results with the large circular island in the previous section. Zooming in and observing the velocity vectors, a single vortex arises, rather than a vortex street-like pattern. Besides the vortex a trail is also visible, which is where the “tail” of the vortex meets the general flow stream, resulting in a swirl periodically resembling a snail house. Observing the results over time, a vortex appears behind the island (relative to flow) and moves around. It gradually disperses when the tide changes, after which it arises again at the other side of the island. Here too, the velocities at the flanks of the island increase such that the area of the Ballonplaat between the island and the fairways at the north and south side reaches similar velocities as in the fairways. Locally, these speeds can go up to 1 – 1.2 m/s very close to the island. This, compared to the earlier observed velocities at P6 of 0.5 – 0.8 m/s in section 4.2.2 for the case without island, for this timestamp.

5.2.2 E-W orientated large half ellipse shaped island

The results for this scenario also show a distinct difference to the large circular island, as well as the N-S orientated half ellipse, as shown in Figure 20. This scenario is considered as the more favourable orientation because the island is positioned roughly parallel to the general flow direction. When looking at the figures, the darker area does seem to have a less turbulent pattern than the previously simulated cases. Especially when it is flood tide, the low velocity area looks like a straight streak. When it is ebb tide, a wake similar to the shape of the island starts to develop at some point. It is likely that this difference in shape is mostly due to the fact that the island was not positioned exactly perpendicular to the direction of the flow.

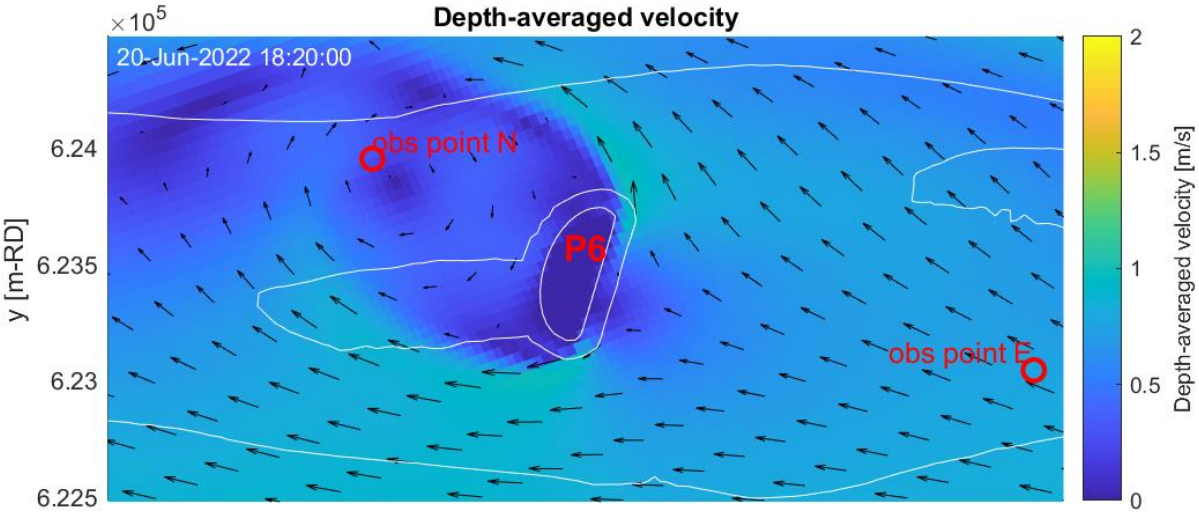

Figure 19 Depth-averaged velocity results for the large ellipse shaped island orientated N-S.

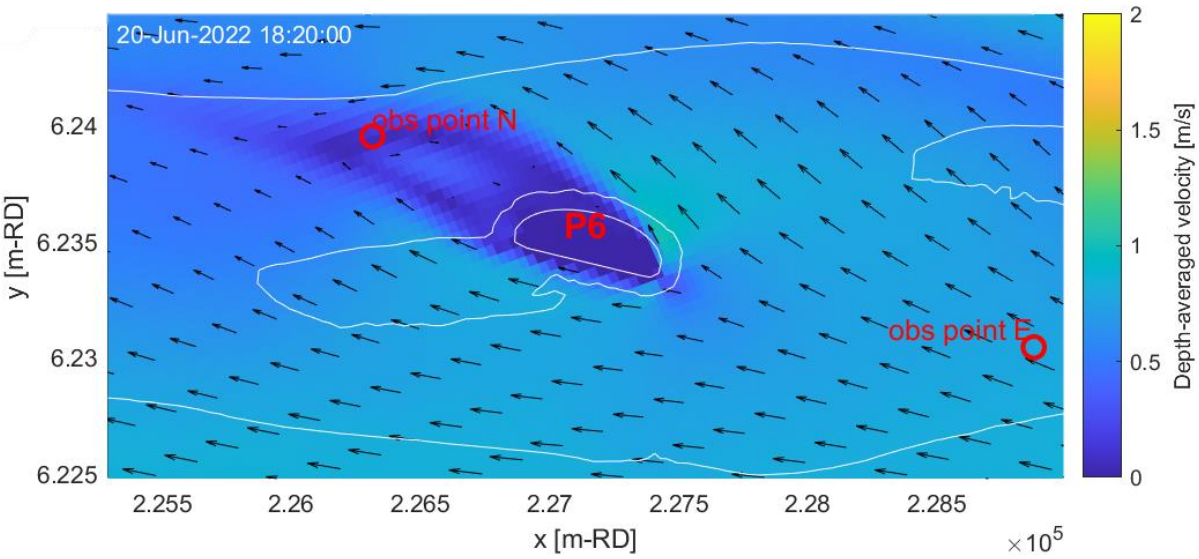

Figure 20 Depth-averaged velocity results for the large ellipse shaped island orientated E-W.

5.3 EFFECT OF WAVES ON THE DEPTH-AVERAGED VELOCITY

The same island configuration as in the previous section is used with the large half ellipse N-S and E-W orientated. However, this time waves are added to the simulation. By adding waves to the model, a comparison can be made between the depth-averaged velocities for the half ellipse shaped island with and without waves.

The addition of waves to the model also has an influence on the resulting depth-averaged velocity because of the processes discussed earlier in sections 2.2 and 4.3. Especially wave breaking will cause increased velocities locally.

When plotting the difference in depth-averaged velocity between the case with and without added waves, results appear over the whole area (Figure 21). The addition of waves to the model is showing generally reduced velocities in shallower areas, while velocities increase in deeper areas like the fairways north and south of the island. However, at times, the area stretching from the west side of the island over the Ballonplaat shows quite increased velocities reaching up to an increase of about 1 m/s.

Generally, a similar result is obtained for both the N-S and E-W orientated islands. Though, when focusing on the area directly around the island, some differences can be seen which would make the N-S orientation less desirable. Looking closely at the area slightly above observation point E (Figure 21), the N-S island induces higher velocities in that area, while this does not happen for the E-W island.

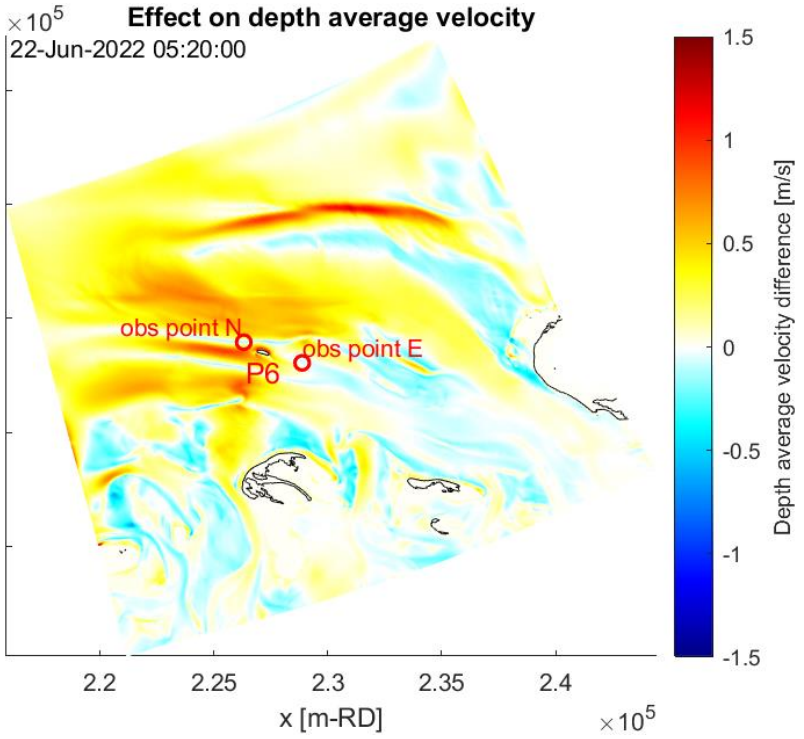

Figure 21 The difference in depth average velocity between the addition of waves and no waves for the half ellipse shaped island orientated E-W.

5.4 EFFECT OF THE ADDITION OF AN ISLAND

Finally, to determine the effect of the addition of an island, a comparison of the significant wave height for the no island case and the ellipse shaped islands is made. Additionally, comparison plots for the depth-averaged velocities are also created. For both comparisons, the computed results without island are subtracted from the computed results with the ellipse shaped islands, for storm conditions.

5.4.1 Significant wave height

In addition to comparing the differences between the results with and without waves, the significant wave height in the current situation (as shown in section 4.2.1) can also be compared to the resulting significant wave height after the addition of an island (Figure 22). The results for the ellipse shaped island orientated N-S and E-W with an offshore wave of 7 m have both been compared to the current situation. Wave heights mainly decreased with up to 1 – 1.5 m in the shadow zone close to the island, while decreasing with around 0.5 m in the shadow zone farther from the island in southeast direction. It is interesting to see how far the trail of reduced wave heights extends, stretching over 7 km to the southeast from the island. This is the shadow zone of the island since the waves generally come from the opposite direction of the island as the trail. Comparing the computed wave height differences for the N-S orientated island with E-W it is observed that, while the wake zone close to the island shows differences due to the different orientations of the islands, they resemble each other further southeast-ward form the island.

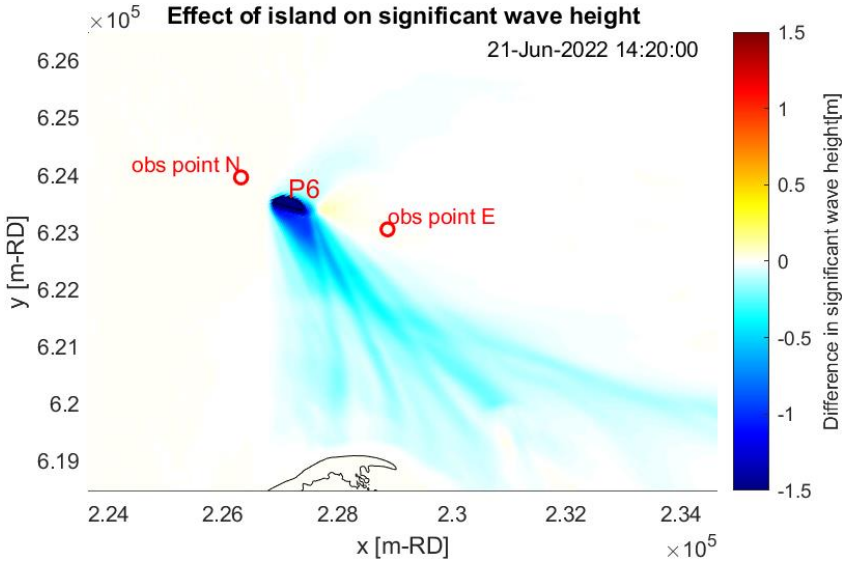

Figure 22 The difference in significant wave height between the current situation without island and the E-W orientated ellipse shaped island, for storm waves of 7 m with a period of 13 s.

5.4.2 Depth-averaged velocity

As could already be seen in the results of sections 5.1 and 5.2, the addition of an island is quite impactful on the flow patterns in the surrounding areas. To emphasize the effects, difference plots have been made for the case without island and both orientations of the ellipse shaped island, shown in Figure 24. The shown snapshot is when the differences between the island and no island case appear the greatest. For storm conditions, locally on the flanks of the island an increase of nearly 1 m/s can be seen for both orientations. In certain areas, the current velocities decrease, such as in parts of the shadow zone behind the island, where the velocities drop with respect to the situation without island. This region 'flips' as a result of the tidal flow direction (flood versus ebb).

Overall, the effects of the N-S orientated island are predicted to be more severe. This does not necessarily relate to the magnitude of the differences in depth-averaged velocity, but rather its spatial coverage, which can be deduced from the more colourful plot in Figure 23 compared to Figure 24. This makes sense, because the N-S orientated island covers more area, with respect to the tidal flow direction, and therefore disrupts the flow on a larger area. This is compared to the E-W orientated island, which is positioned in a more streamlined orientation.

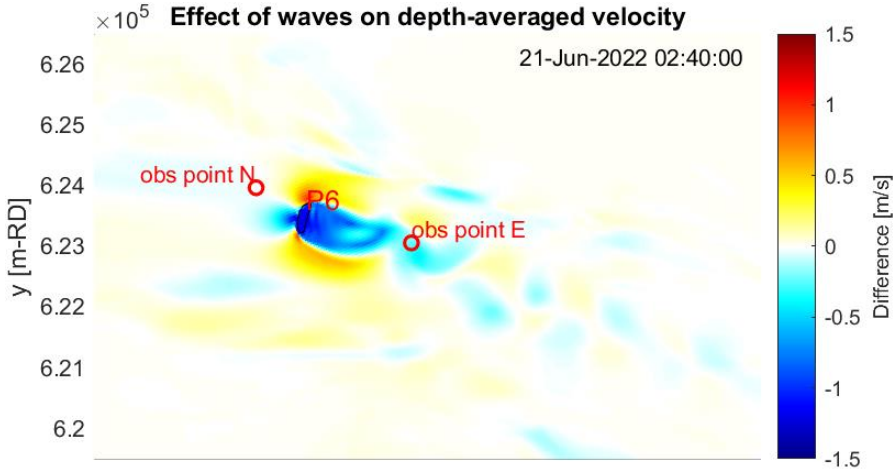

Figure 23 The difference in depth-averaged velocity between the current situation without island and the N-S orientated ellipse shaped island, for storm waves of 7 m with a period of 13 s.

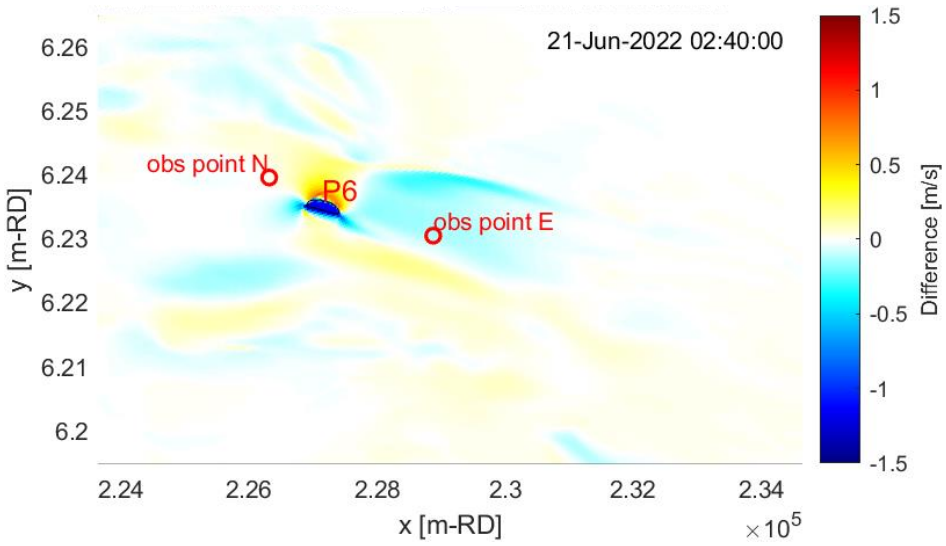

Figure 24 The difference in depth-averaged velocity between the current situation without island and the E-W orientated ellipse shaped island, for storm waves of 7 m with a period of 13 s.

5.5 COMPARISON TO 1D THEORETICAL WAVE MODEL

To see whether the addition of an island has a big influence on the results for the 1D models, another comparison is done on the models as in the previous chapter.

Real profile with island

The same setup is used as for the real profile without island in chapter 4.3, in terms of cross-sectional distance and step size.

Figure 25 shows the computed wave heights close to the island location. At first glance there does not appear to be too big of a difference to the case without island and the island with a slope of 1:1.5. The results now resemble the theoretical case since the slope of the island is linear. In both cases, Model 1 and 3 show a similar shape in the results, with Model 1 relatively underestimating the wave height. Interestingly, what could already be seen in the case without island, Model 2 drops under Model 1 and 3 when approaching the island/shallow area after initially predicting higher waves than the other two models for the year-round waves. Different from the case without island though is that the results of Model 2 converge with Model 1 and 3, instead of relatively overestimating the wave height all the way through for the storm wave case.

The island with a combined slope of 1:1.5 from deep water until 0 m NAP and 1:6 from 0 m NAP to 5 m NAP gives very similar results to the first island case. However, this is to be expected since the slope for both cases is the same until 0 m NAP. The main differences are in the results of Model 3, which shows higher peaks before the waves break in both wave scenarios, but especially for storm waves.

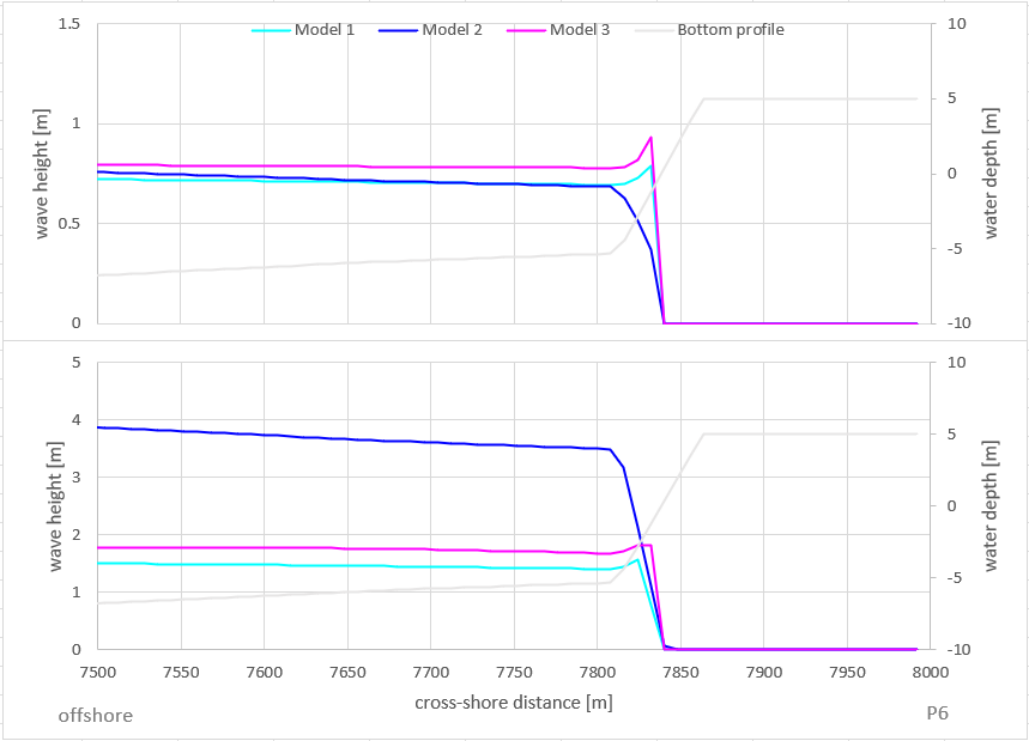

Figure 25 Results of the 1D wave models for the real bathymetry with island (slope 1:1.5) with year-round waves (top), and storm waves (bottom)

It is within expectations that the effect of the island on the wave height is so small. The length of the cross-section over which the wave heights were computed is much larger than the island itself, comparing a cross-section of nearly 8 km to an island of order 500 m. The island is very small compared to the area, and considering there was already little wave height variation over time without island, the addition of an island would not induce any grand changes. A visualization of the scale of the island compared to the cross-section can be found in appendix Cii.

6. CONCLUSIONS AND RECOMMENDATIONS

Conclusions

In this section, the research questions are answered based on the findings of this study.

1. What are the current morphological and hydrodynamic conditions in the area without an artificial island?

From literature research, it has become clear that the study area in general is quite dynamic. This means that, locally, the seabed level underwent changes of up to 10 m in about 40 years. This is especially due to the migration of tidal channels, including the main navigation channel (Westereems) to Eemshaven. However, the western part of the Ballonplaat, which is the shoal on which the small energy island is planned to be built, seems to have been quite stable over the past.

The hydrodynamic situation is governed by (storm) waves and tidal currents in the area. Extreme waves from the northwest exceeding 7 m in height are not uncommon. During flood tide the currents near the Ballonplaat are generally going to the east and during ebb tide the flow is oriented to the west.

2. What are possible designs for an island and which island features can be distinguished and varied?

Several island designs were made, which were mainly based on various shapes. Other features that have been included in the design are the location, size, orientation, height, and slope. A selection of possible island designs was made for which computations with a numerical model were performed to assess the effects of the island on the hydrodynamics.

3. How is the Delft3D-SWAN model constructed and what are the main model settings?
    a. Which assumptions are being made?

Assumptions that have been made include depth-averaging the flows, constant salinity, uniform hydraulic roughness, JONSWAP spectrum based waves, and the exclusion of wind effects.

    b. How can an artificial island be added into Delft3D/SWAN?

An island can be added to the Delft3D/SWAN model by first using a program which, by specifying all the relevant island parameters, converts the island contours into an xyz points file. This file can then be added into Delft3D QUICKIN and transformed into a depth file using triangular interpolation, after which it can be combined with an existing bathymetry file of the area without island. In this way, the constructed island design is implemented at the location of interest (in this study mainly at 2 locations on the western part of the Ballonplaat, referred to as P1 and P6).

    c. How does the SWAN model compare to a theoretical wave model?

The comparison of the wave heights computed with the 2-D SWAN model and the theoretical 1D wave models showed some differences in results. For the year-round waves, the resulting wave heights obtained through the 1D models deviated up to about 0.1 m over the cross-section, but up to 0.2 m near the P6 location. For the storm waves this was up to 2 m throughout the cross-section, but up to 0.1 m close to the P6 location. However, besides the 2D SWAN model being able to include more processes in the computation of the wave height, it should also be noted that the Ursell parameter turned out to be too high for the storm waves, indicating that linear wave theory was not applicable during these storm conditions, hence suggesting that the 1D models based on linear wave theory are not accurate.

4. What are the hydrodynamic responses in the study area resulting from the addition of an island and which island feature is most influential in affecting the hydrodynamics?

General

To answer this research question, use was made of the output of coupled Delft3D-SWAN simulations for both the situation without an island and for the case with a given island design. To drive the models, 2 conditions were considered: offshore year-round waves with a significant height of 1 m and storm waves of 7 m, coming from the northwest.

Current situation (without island)

During year-round wave conditions, the computed depth-averaged current velocities around the P6 location are approx. 0.9 m/s and wave heights are about 1 m. During storm conditions, velocities around P6 were computed to be about 1.4 m/s and wave heights of up to around 3 m.

Situation with island

To answer the first part of the research question, the addition of an island resulted in clear changes in the depth-averaged velocities as well as in the significant wave heights in the vicinity of the island. For storm conditions, the depth-averaged velocities increase with a maximum of about 1 m/s along the flanks of the island. In certain areas, the current velocities decrease, such as in parts of the shadow/wake zone behind the island, where the velocities drop with respect to the situation without island. This region 'flips' as a result of the tidal flow direction (flood versus ebb). Additionally, the results for significant wave heights during storm conditions show that these mainly decreased with up to 1 – 1.5 m in the shadow zone close to the island, while decreasing with around 0.5 m in the shadow zone farther from the island in South-East direction. Plotting the differences in hydrodynamics (depth-averaged velocity and significant wave height) between the case with and without island, showed that the predicted effects of the island could reach over 10 km distance from the island location for storm conditions.

Effects of island parameters

Size

The Delft3D model results show that even a small island had quite an impact on the flow patterns directly in the area. The small circular island induced vortex shedding, leading to the appearance of a pattern resembling a vortex street stretching for several kilometres periodically. The size of the island seemed to be a "limiting" factor for this phenomenon, as the large island size relative to the Ballonplaat shoal restricted the formation of a large number of vortices in the vortex street.

Shape

Furthermore, the shape of the island also has a significant impact on the flow patterns. When comparing the circular island to the N-S orientated half ellipse shaped island, the width of the island (with respect to the flow direction) was similar in both cases. However, the latter island shape is flatter and has a straight side, creating a similar flow pattern but the wake is wider because the island is less streamlined than the circular shape. The opposite is the case for the E-W orientated ellipse shaped island, where the flow pattern is no longer showing vortices, thus indicating that the effects of the shape of the island also really depends on its orientation (see below).

Orientation

Next to shape, the orientation of a non-circular island has significant impact on the flow patterns behind the island (relative to the tidal flow direction). This was very apparent from the computed results for an elongated shape, where for an island with a more N-S orientation, the flow is much more obstructed, yielding large shadow zones and associated accelerations near the island flanks. The orientation did not seem to influence the significant wave height pattern much, though local differences are obviously found due to differences in blocking/refraction.

Governing island parameter

From the study, it appeared that many island parameters affect the hydrodynamics of the surrounding areas. All three island parameters size, shape and orientation have a major influence on current and wave patterns and the ranking of their effects cannot be established easily. This is mainly because the parameters are so interlinked to each other, that it becomes difficult to recognize each individual contribution.

Recommendations

Based on the results from this research, some recommendations regarding the design of the island, as well as future research are proposed in this section.

Firstly, the shape and orientation of the island that is recommended is a streamlined, slightly elongated island shape (not circular), oriented such that it is most aligned with the Ballonplaat shape and the main tidal flow direction. From the Delft3D-SWAN simulations, this configuration resulted in less impact on the hydrodynamics in the area compared to other configurations.

Next, some recommendations are given on the modelling. It is recommended to verify the computed waves with both the 2-D SWAN and 1-D theoretical models with wave measurements. Additionally, it is recommended to assess the effects when including varying flow velocities over the water column (3-D model) and to add wind effects on the water levels (and currents). Furthermore, it could be interesting to further look into the underlying differences between the theoretical 1D wave model. In addition, though computationally heavy, decreasing the grid size of the Delft3D-SWAN model could also increase the model accuracy, especially close to the island. This will also allow to investigate the effects of the varying island slopes in more detail (for example, the effects of wave reflection).

Finally, to extend the prediction of the effects of an artificial island, important aspects to investigate are the effects of the island on the sediment transport patterns as well the morphological developments of the area. This would really determine what the lasting effects of such an island are, or whether building an island in that area is feasible at all.

7. REFERENCES

Battjes, J., & Janssen, J. (1978). Energy loss and set-up due to breaking random waves. Hamburg: ASCE.

Chee, S., Othman, A., Sim, Y., Mat Adam, A., & Firth, L. (2017). Land reclamation and artificial islands: Walking the tightrope between development and conservation. *Global Ecology and Conservation, 12*, pp. 80-95. doi:doi.org/10.1016/j.gecco.2017.08.005

Deltares. (1999). *Assessment of morphological impacts due to construction of artificial islands along the coast of Israel.*

Deltares. (2022). Delft3D-FLOW User Manual. Retrieved from https://content.oss.deltares.nl/delft3d/manuals/Delft3D-FLOW_User_Manual.pdf

EUMeTrain. (2017). *Kármán Vortex Streets*. Retrieved from EUMeTrain: https://resources.eumetrain.org/data/4/452/navmenu.php?tab=8&page=1.0.0

Grashorn, S., Lettmann, K., Wolff, J., Badewien, T., & Stanev, E. (2015, February). East Frisian Wadden Sea hydrodynamics and wave effects in an unstructured-grid model. *Ocean Dynamics*, pp. 419-434.

Kaneko, S., Nakamura, T., Inada, F., & Kato, M. (2008). Vibration Induced by Cross-Flow. In *Flow Induced Vibrations* (pp. 29-106). Elsevier.

Lam, K., & Dai, G. (2002, October). Formation of vortex street and vortex pair from a circular cylinder oscillating in water. *Experimental Thermal and Fluid Science*, pp. 901-915.

Liu, G., Qi, H., Cai, F., Zhu, J., Zhao, S., Liu, J., . . . Xiao, Z. (2022). Initial morphological responses of coastal beaches to a mega offshore artificial island. *Earth Surface Processes and Landforms, 47*(6), pp. 1355-1370.

Mahmoodian, M., & Egon, A. (2010). A Review of Construction of artificial islands. *PORTS2010.* Florida.

RHDHV. (2021). *Rapportage Onderzoek Innovatie Doorkruising Waddengebied.*

Rijkswaterstaat. (n.d.). *Uitleg over Golven*. Retrieved November 2022, from knmi: https://www.knmi.nl/kennis-en-datacentrum/uitleg/golven#:~:text=Langs%20de%20Waddenkust%20zijn%20golven,de%20lucht%20en%20het%20water.

Rijkswaterstaat. (n.d.). *Waterhoogte Astronomisch t.o.v. NAP*. Retrieved November 2022, from waterinfo.rws: https://waterinfo.rws.nl/?#!/details/publiek/astronomische-getij/Huibertgat(HUIBGT)/Waterhoogte___20berekend___20Oppervlaktewater___20t.o.v._ __20Normaal___20Amsterdams___20Peil___20in___20cm

State of Green. (2021, January). *This is what the world's first energy island may look like*. Retrieved from stateofgreen.com: https://stateofgreen.com/en/news/this-is-what-the-worlds-first-energy-island-may-look-like/

The Danish Energy Agency. (n.d.). *Denmark's Energy Islands*. Retrieved November 2022, from https://ens.dk/en/our-responsibilities/energy-islands/denmarks-energy-islands

van der Werf, J. (2021, August). Syllabus Wave-Dominated Coastal Dynamics. Voorburg.

van der Werf, J. (2021-2022). Wave Dominated Coastal Dynamics 2021-2022 Group assignment.

van Rijn, L. (2011). *Principles of fluid flow and surface waves in rivers, estuaries, seas and oceans.* Aqua Publications.

wadkanovaren.nl. (2021). *De dynamiek van het Wad*. Retrieved from https://wadkanovaren.nl/

WaterProof. (2021). *Gemini Export Cables (Draft version).*

WaterProof. (2022). *Optimal OWF export cable route alternatives towards Eemshaven.*

APPENDICES

A. ISLAND VARIANTS

An overview of the island scenario variants is shown in the table below. The orientation of the elongated shape was adjusted to align with the general direction of the water flow in the area for option A, and transversal on the flow for option B. The degrees listed are the angles with respect to the north based on a horizontal orientation of the rectangular shape (base orientation E-W), and for the halfmoon and ellipse shapes based on vertical orientation with the straight quay of the halfmoon to the east.

Table 4 Island scenario variants

Variant	Location	Size	Shape	Orientation	Height	Slope	Comments
1	A	A	A	-	A	A	
2	A	B	A	-	A	A	
3	B	A	A	-	A	A	
4	B	B	A	-	A	A	
P6o15S	B	A	B	A(15degN)	A	A	Min effect
P6o15L	B	B	B	A(15degN)	A	A	
P6n285S	B	A	B	B(285degN)	A	A	
P6n285L	B	B	B	B(285degN)	A	A	Max effect
P1C1o285S	A	A	C	A(285degN)	A	A	Min effect
P1C1o285L	A	B	C	A(285degN)	A	A	
P1C1n15S	A	A	C	B(15degN)	A	A	
P1C1n15L	A	B	C	B(15degN)	A	A	Max effect
P6C1o285S	B	A	C	A(285degN)	A	A	Min effect
P6C1o285L	B	B	C	A(285degN)	A	A	
P6C1n15S	B	A	C	B(15degN)	A	A	
P6C1n15L	B	B	C	B(15degN)	A	A	Max effect
P6C1o105L	B	B	C	A(105degN)	A	A	
ellipsP6t15	B	B	D	A(110degN)	A	A	Nr in name based on slope
ellipsP6t1-5	B	B	D	A(110degN)	A	B	idem
Ellips1-5	B	B	D	A(110degN)	B	C	Contour at 0 m NAP
Ellips1-6	B	B	D	A(110degN)	B	C	idem

B. TIMESERIES CORRESPONDING TO AREA PLOTS

Significant wave height corresponding to Figure 10

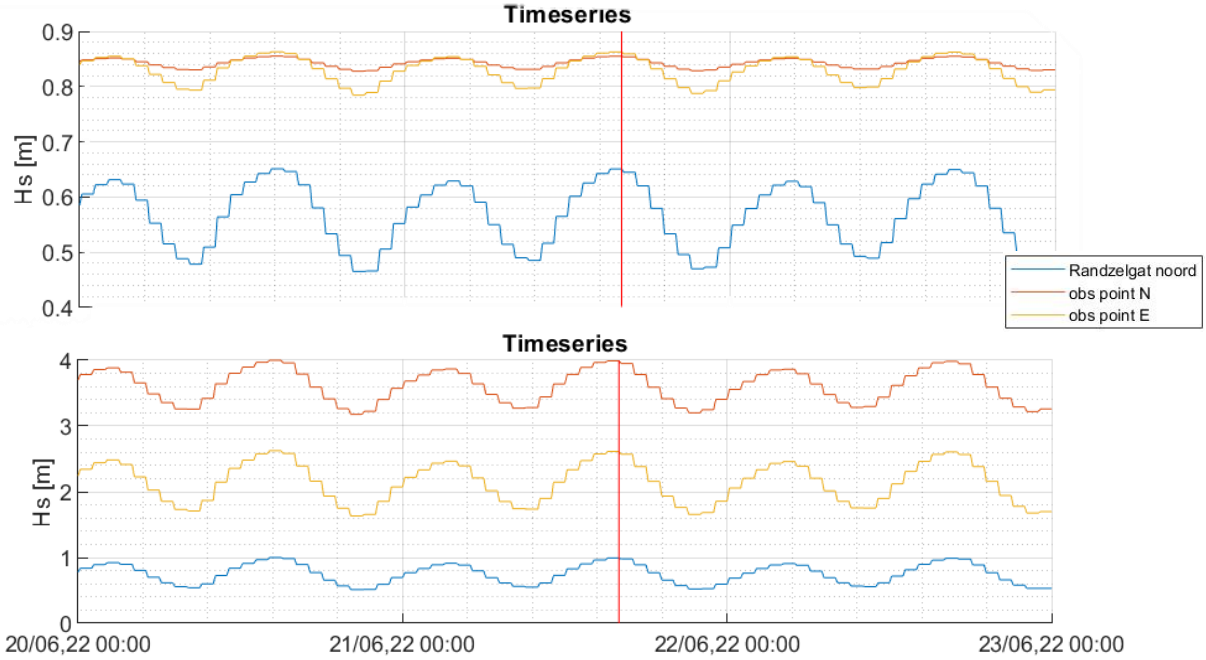

C. THEORETICAL 1D WAVE MODEL

i. Realistic bathymetry based on cross-sections 2 & 3

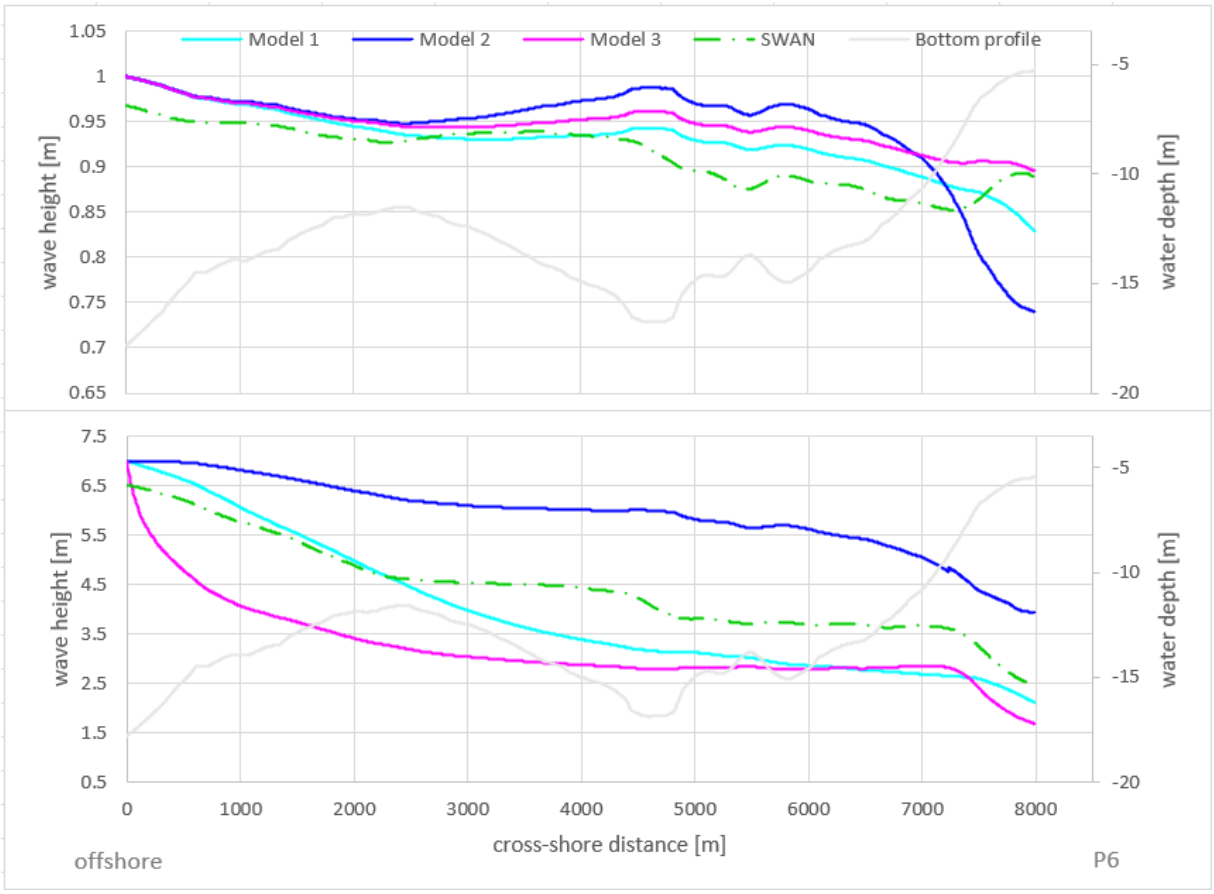

Figure 26 Wave height results of the 1D wave models and SWAN for cross-section 2 without island based on year-round waves (top), and storm waves (bottom)

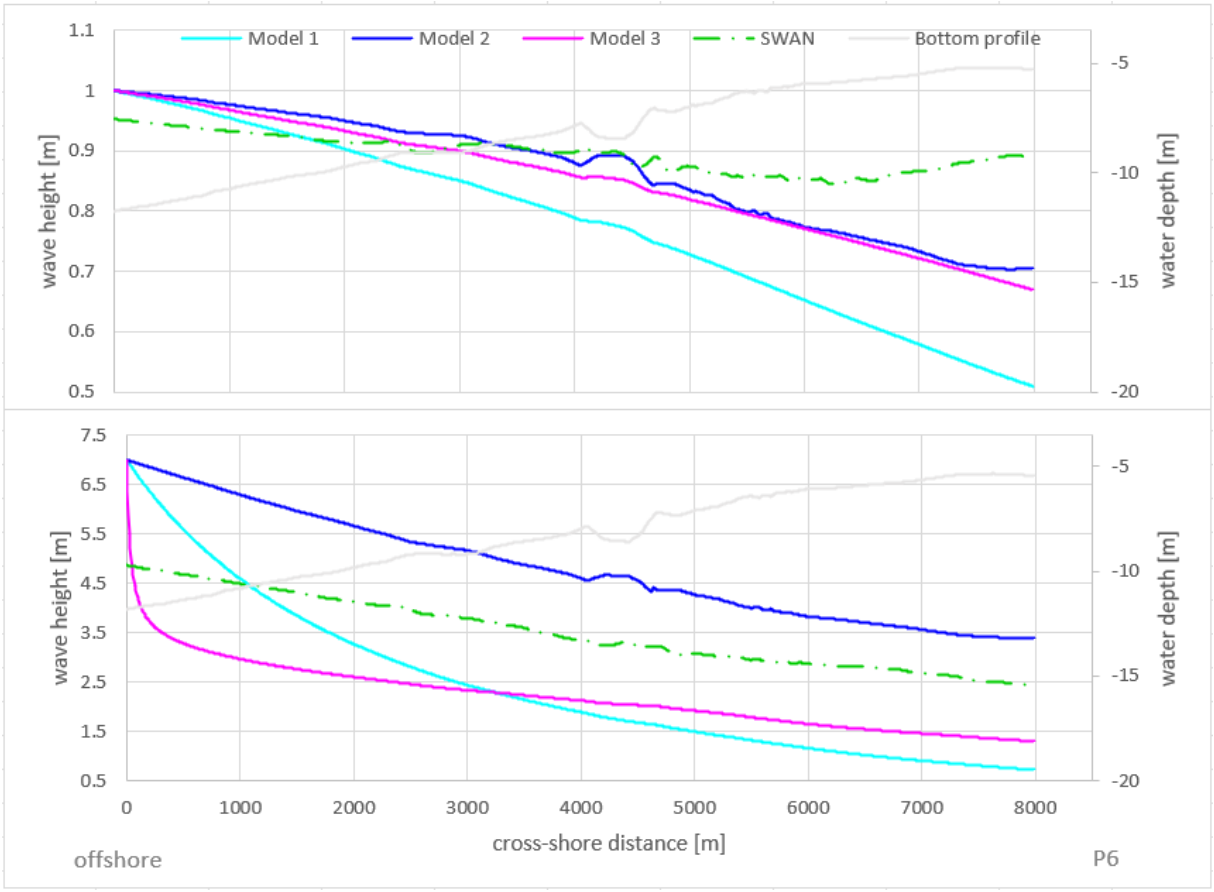

Figure 27 Wave height results of the 1D wave models and SWAN for cross-section 2 without island based on year-round waves (top), and storm waves (bottom)

ii. Island location with respect to cross-section

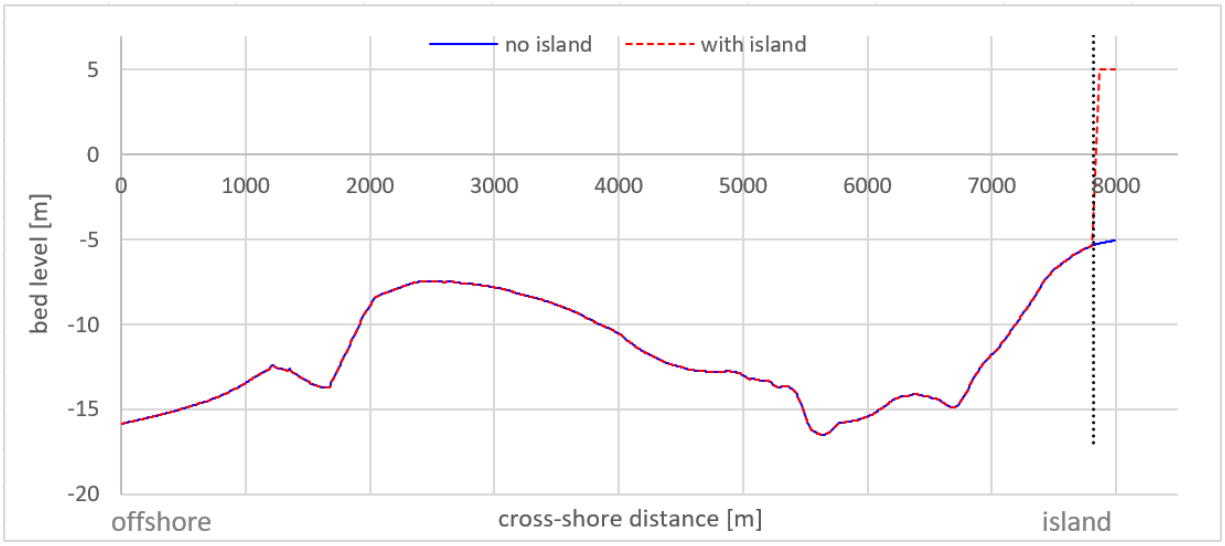

Figure 28 Cross-section 1 with possible island indication